

Comparing Sequential Forecasters

Yo Joong Choe, Aaditya Ramdas
Department of Statistics and Data Science
Machine Learning Department
Carnegie Mellon University
yjchoe@cmu.edu, aramdas@cmu.edu

October 4, 2021

Abstract

We consider two or more forecasters each making a sequence of predictions over time and tackle the problem of how to compare them — either online or post-hoc. In fields ranging from meteorology to sports, forecasters make predictions on different events or quantities over time, and this work describes how to compare them in a statistically rigorous manner. Specifically, we design a nonasymptotic sequential inference procedure for estimating the time-varying difference in forecast quality when using a relatively large class of scoring rules (bounded scores with a linear equivalent). The resulting confidence intervals can be continuously monitored and yield statistically valid comparisons at arbitrary data-dependent stopping times (“anytime-valid”); this is enabled by adapting recent variance-adaptive confidence sequences (CS) to our setting. In the spirit of Shafer and Vovk’s game-theoretic probability, the coverage guarantees for our CSs are also distribution-free, in the sense that they make no distributional assumptions whatsoever on the forecasts or outcomes. Additionally, in contrast to a recent preprint by Henzi and Ziegel, we show how to sequentially test a *weak* null hypothesis about whether one forecaster outperforms another on average over time, by designing different e-processes that quantify the evidence at any stopping time. We examine the validity of our methods over their fixed-time and asymptotic counterparts in synthetic experiments and demonstrate their effectiveness in real-data settings, including comparing probability forecasts on Major League Baseball (MLB) games and comparing statistical postprocessing methods for ensemble weather forecasts.

Contents

1	Introduction	3
1.1	Related Work	4
2	Preliminaries	6
2.1	Martingales, Ville’s Inequality, and Confidence Sequences	6
2.2	Proper Scoring Rules	7
3	Confidence Sequences for Forecast Score Differentials	8
3.1	A Game-Theoretic Motivation	8
3.2	The Formal Setup	9
3.3	Scoring Rules with Linear Equivalents	10
3.4	Time-Uniform Confidence Sequences for Δ_t	10
3.4.1	Time-uniform Boundaries and Exponential Supermartingales	10
3.4.2	Warmup: Hoeffding-Style Confidence Sequences for Δ_t	11
3.4.3	Main Result: Empirical Bernstein Confidence Sequences for Δ_t	12
3.4.4	Choosing the Uniform Boundary u	13
3.5	e-Processes and Anytime-Valid p-Processes	14
4	Extensions	17
4.1	Probabilistic Forecasts on Categorical Outcomes	17
4.2	k -Step-Ahead Forecasts	19
4.3	Mean Forecasts on Bounded Continuous Outcomes	20
4.4	Winkler’s Normalized Score Differentials	21
5	Experiments	22
5.1	Simulated Experiments	22
5.2	Comparing Forecasters on Major League Baseball Games	28
5.3	Comparing Statistical Postprocessing Methods for Weather Forecasts	32
6	Conclusions	35
A	Tight Confidence Sequences via Uniform Boundaries	40
B	Proofs	40
B.1	Proof of Lemma 3.1	40
B.2	Proof of Theorem 3.2	40
B.3	Proof of Theorem 3.3	41
B.4	Proof of Lemma 4.1	42
B.5	Proof of Lemma 4.2	43
C	Computing the Gamma-Exponential Mixture	43
D	Comparing CS Widths on IID Means	45

1 Introduction

Forecasts of future events and quantities are widely used in many domains, including meteorology, economics, epidemiology, elections, and sports. Often, we are given a set of forecasts made by different forecasters on a regularly occurring event, such as whether it will rain tomorrow and whether a sports team will win its next game. Other times, we are provided with forecasts on a future quantity across a time period, such as the number of weekly hospitalizations and deaths during a pandemic, the value of a stock market index, and the voter turnout.

Despite the popularity of forecasts across many domains, it is not obvious how we can evaluate and compare different forecasters on their predictive ability over time, as data is sequentially observed and the forecasts are subsequently updated. As an illustrative example, consider various game-by-game predictions made on the outcome of the 2019 World Series by real-world forecasters in Table 1. The outcome of a baseball game is clearly difficult to predict or model across time; furthermore, we also do not have full information on how the forecasts are generated. Had we been interested in determining which forecaster to trust going into the next game, how can we find out if one (if any) forecaster is better than another for predicting the winner of the next game? More generally, how do we determine that one forecaster is better than another at predicting the next outcome at *any* given time point, without having to make assumptions about how the reality behaves or how the forecasts are made?

In this work, we derive a statistically rigorous procedure for sequentially comparing the performances of such probability forecasts, using the powerful tool of *time-uniform confidence sequences (CS)* (Darling and Robbins, 1967; Lai, 1976b; Howard et al., 2021). CSs are sequences of confidence intervals that provide time-uniform and non-asymptotic coverage guarantees, enabling valid sequential inference at any stopping time for a time-varying parameter of interest, such as the difference in the average predictive performance up to time t . In particular, the coverage guarantees are valid both in the cases where inference is done sequentially after each outcome and in the case of post-hoc inference on the (sequentially) observed data.

We motivate our derivation of confidence sequences by introducing a game-theoretic setup (Shafer and Vovk, 2019), in which two players play a sequential forecasting game on an outcome with an unknown parameter. This game highlights the sequential nature of the problem setting and the need for a time-uniform and distribution-free inference procedure. We then use the martingale theory of scoring rules with linear equivalents (Lai et al., 2011) to derive confidence sequences for the time-varying difference in average forecasting scores of the two forecasts. The resulting sequential inference procedure is time-uniform, non-asymptotic, and also distribution-free: we make virtually no assumptions on how the outcomes (and forecasts, in most cases) are actually generated.

The rest of the paper is organized as follows. After discussing related work in Section 1.1 and preliminaries in Section 2, in Section 3, we derive CSs for the time-varying average forecast score differentials between two probability forecasters on binary outcomes. In Section 3.5, we also derive *e-processes* and *anytime-valid p-processes* (Ramdas et al., 2020) as duals to our CSs that provide alternative sequential inference procedures for forecast comparison. In Section 4, we discuss extensions of our CSs, including the cases of categorical and bounded continuous outcomes as well as k -step-ahead forecasts. In Section 5.1, we empirically validate our CSs and compare them against fixed-time and asymptotic confidence intervals (CIs) on simulated data. Finally, in Sections 5.2 and 5.3 we apply our methods to real-world forecast comparison tasks, namely comparing game-by-game predictions in Major League Baseball (MLB) and comparing statistical postprocessing methods of ensemble weather forecasts.

Forecasts on Nationals Win	1	2	3	4	5	6	7
FiveThirtyEight ¹	38%	41%	53%	59%	37%	41%	48%
Vegas-Odds.com ²	35%	38%	41%	51%	34%	37%	43%
Adjusted Win Percentage	47%	48%	47%	47%	47%	47%	47%
K29 Defensive Forecast	53%	55%	56%	54%	52%	50%	52%
Constant Baseline	50%	50%	50%	50%	50%	50%	50%
Average Joe	40%	50%	60%	50%	30%	40%	50%
Nationals Fan	70%	70%	80%	70%	60%	60%	70%
Did the Nationals Win?	Yes	Yes	No	No	No	Yes	Yes

Table 1: Probability forecasts (%) on whether the Washington Nationals will win each game of the 2019 World Series. The first two forecasts are taken from publicly available websites online. The next three forecasts are baselines computed using the 10-year win/loss records (win probability is rescaled with the opponent’s win probability to sum to 1; see Section 5.2 for more details). The last two forecasts are imaginary (but not unrealistic) casual sports fans making their own forecasts using different heuristics. All forecasts are made prior to the beginning of each game. See Section 5.2 for more details on the forecasting methods and comparisons.

1.1 Related Work

Evaluation and Comparison of Probability Forecasts. Evaluation of probability forecasts is a well-studied subject in the literature of statistics, economics, finance, and climatology, dating back to at least the works of Brier (1950); Good (1952); DeGroot and Fienberg (1983); Dawid (1984); Schervish (1989). Many of the work on scoring rules focus on the properties of forecasts induced by these scoring rules, namely calibration and the sharpness of probability forecasts. See Gneiting and Raftery (2007); Winkler et al. (1996); Gneiting et al. (2007) for in-depth reviews of the subject.

The problem of comparing probability forecasts while accounting for sampling uncertainty was first popularized by Diebold and Mariano (1995) (DM), who proposed tests of equal (historical) forecast accuracy using the differences in forecast errors. The DM test is based on the asymptotic normality of the average forecast score differentials, and it makes stationarity assumptions about the outcomes. Giacomini and White (2006) (GW) developed tests of *conditional* predictive accuracy given past information, allowing for the comparison of “which forecaster will be more accurate at the forecast target date” rather than which one performed better in the past. The GW test thus allows for nonstationarity, although its validity depends on mixing and moment assumptions. Lai et al. (2011) presented a comprehensive overview of the aforementioned methods of forecast comparison and develops a martingale-based theory of scoring rules that have linear equivalents, such as the Brier score and the logarithmic score. They proved the asymptotic normality of both forecast scores and score differentials, leading to an asymptotic CI that we use as a point of comparison in our work. While the theory in Lai et al. (2011) is a building block for our work, the key difference is that we depart from the classical notions of asymptotic and fixed-size CIs, and instead develop asymptotic and non-asymptotic CSs that are valid at arbitrary stopping times, all while making virtually no assumption made on the data generating distribution.

¹Source: <https://projects.fivethirtyeight.com/2019-mlb-predictions/games/>.

²Source: <https://sports-statistics.com/sports-data/mlb-historical-odds-scores-datasets/>.

Method & Key Result	Null (Implied or Stated)	ST	NA	DF
Diebold and Mariano (1995) $\sqrt{t}(\hat{\Delta}_t - \mu) \rightsquigarrow N(0, 2\pi f_d(0))$	$H_0 : \mathbb{E}[\hat{\delta}_t] = 0$	✗	✓/✗	✗ (stationarity)
Giacomini and White (2006) $T_m(\hat{\delta}_t) \rightsquigarrow \chi^2$ (m : window size)	$H_0 : \mathbb{E}[\hat{\delta}_t \mathcal{F}_{t-1}] = 0$	✗	✗	✗ (mixing)
Lai et al. (2011) $\sqrt{t}(\hat{\Delta}_t - \Delta_t)/s_t \rightsquigarrow N(0, 1)$	$H_0 : \mathbb{E}[\hat{\delta}_t \mathcal{F}_{t-1}] = 0$	✗	✗	✓
Ehm and Krüger (2018) $\frac{1}{\sqrt{t}} \sum_{i=1}^t \sigma_i \hat{\delta}_i(\theta) \rightsquigarrow N(0, \gamma(\theta))$, ($\sigma_i = \pm 1$ w.p. $\frac{1}{2}$ each)	$H_0^w : \frac{1}{\sqrt{t}} \sum_{i=1}^t \mathbb{E}[\hat{\delta}_i(\theta) \mathcal{F}_{i-1}] = 0$ $H_0^s : \mathbb{E}[\hat{\delta}_i(\theta) \mathcal{F}_{i-1}] = 0, \forall i \leq t$	✗	✗	✗ (Lindeberg condition)
Henzi and Ziegel (2021) $E_t(\lambda) = \prod_{i=1}^t E_i(\lambda)$ is an e-value, where $E_i(\lambda) = 1 + \lambda \frac{\hat{\delta}_i}{ T(p_i, q_i) }$	$H_0^s : \mathbb{E}[\hat{\delta}_i(\theta) \mathcal{F}_{i-1}] \leq 0, \forall i \leq t$	✓	✓	✓
Ours $t(\hat{\Delta}_t - \Delta_t)$ is sub- ψ (upper-bounded by a NSM)	$H_0^w : \Delta_t = \frac{1}{t} \sum_{i=1}^t \mathbb{E}[\hat{\delta}_i \mathcal{F}_{i-1}] \leq 0$	✓	✓	✓

Table 2: Comparison of popular inference methods for comparing probability forecasts. This table is meant to be a quick summary only; see referenced paper for the precise definitions, conditions, and guarantees for each method. $\hat{\delta}_t = S(p_t, y_t) - S(q_t, y_t)$ and $\hat{\Delta}_t = \frac{1}{t} \sum_{i=1}^t \hat{\delta}_i$ respectively refer to the pointwise and average score differential between forecasts p_t and q_t against the observation y_t at time t . **ST**: whether the method has a stopping time (or time-uniform) guarantee. **NA**: whether the method has a non-asymptotic guarantee. **DF**: whether the method has a distribution-free guarantee.

Recently, Henzi and Ziegel (2021) constructed sequential tests of conditional forecast dominance based on e-values (Vovk and Wang, 2021; Grünwald et al., 2019; Shafer, 2021). Although these one-sided tests are constructed using e-values and have non-asymptotic guarantees, they test a “strong³ null”, such that rejecting the null only provides evidence that there exists some time point in the sequence where one forecaster is better than the other. Notably, rejecting the strong null gives no evidence of *how often* the forecaster is better than the other. In contrast, our non-asymptotic CSs and e-values provide the more informative evidence of whether one forecaster dominates the other over time, as we consider the average of score differentials across all time steps. We examine this distinction further in both Sections 3.5 and 5.3. Nevertheless, we also note that e-values and confidence sequences are closely related via the underlying framework of nonnegative supermartingales (Ramdas et al., 2020) as well as the game-theoretic statistical framework (Shafer and Vovk, 2019).

Table 2 summarizes the aforementioned methods of forecast comparison. Note that we refer to the time-uniform guarantee as a stopping time guarantee, as the two conditions are in fact equivalent (Ramdas et al., 2020). See Section 3.5 for further details.

Time-Uniform Confidence Sequences. Confidence sequences were developed and formalized by many classical results in statistics (Darling and Robbins, 1967; Robbins, 1970;

³This distinction of strong and weak nulls come from the discussion of randomization experiments in the causal inference literature; see, e.g., Lehmann (1975); Rosenbaum (1995); Wu and Ding (2020). Within the context of sequential forecast comparison, Ehm and Krüger (2018) makes the distinction between tests of average and step-by-step conditional predictive ability, which mirrors that of weak and strong nulls.

Robbins and Siegmund, 1970; Lai, 1976a; Jennison and Turnbull, 1989). In recent years, there has been renewed interest on CSs in problems such as sequential A/B testing (Johari et al., 2015) and best-arm selection in multi-armed bandits (Jamieson et al., 2014; Jamieson and Jain, 2018), where CSs are sometimes referred to as always-valid or anytime confidence intervals. Confidence sequences are also duals to sequential hypothesis tests, analogous to confidence intervals being dual to fixed-time hypothesis tests, and one can further derive a sequence of e-values and anytime-valid p-values given the CSs (more precisely, its underlying exponential process) (Ramdas et al., 2021). In Section 3.5, we make this connection explicit and discuss how our sequential inference approach can also be used to quantify the accumulated evidence against the null (e-process) or to decide whether to reject the null hypothesis while sequentially collecting data (anytime-valid p -process).

The recent work by Howard et al. (2021) is of particular importance in our work, as it develops a class of tight confidence sequences that are uniformly valid over time with non-parametric assumptions and has widths that shrink to zero. This work and its underlying technique of nonnegative supermartingales (NSMs) (Howard et al., 2020; Ville, 1939) has led to several interesting results, including state-of-the-art concentration inequalities for mean estimation (Waudby-Smith and Ramdas, 2020), doubly robust sequential causal inference (Waudby-Smith et al., 2021), and off-policy evaluation for contextual bandits (Karampatziakis et al., 2021). Our work makes the connection between the empirical Bernstein (EB) CSs derived in Howard et al. (2021) and the martingale property of forecast score differentials (Lai et al., 2011), leading to a novel sequential inference procedure for anytime-valid forecast comparison.

2 Preliminaries

2.1 Martingales, Ville’s Inequality, and Confidence Sequences

Let $(\Omega, \mathcal{F}, \mathbb{P})$ be a probability space with filtration $(\mathcal{F}_t)_{t=1}^\infty$, with each \mathcal{F}_t representing the accumulated information up to time $t = 1, 2, \dots$. A sequence of random variables $(X_t)_{t=1}^\infty$ is *adapted* to $(\mathcal{F}_t)_{t=1}^\infty$ if $X_t \in \mathcal{F}_t$ for each t and *predictable* if $X_{t+1} \in \mathcal{F}_t$ for each t . A sequence $(X_t)_{t=1}^\infty$ adapted to $(\mathcal{F}_t)_{t=1}^\infty$ is a *supermartingale* if $\mathbb{E}[|X_t|] < \infty$ and $\mathbb{E}[X_{t+1} | \mathcal{F}_t] \leq X_t$ for each t . $(X_t)_{t=1}^\infty$ is a *submartingale* if $(-X_t)_{t=1}^\infty$ is a supermartingale, and it is a *martingale* if it is both a supermartingale and a submartingale. Moreover, a sequence $(D_t)_{t=1}^\infty$ adapted to $(\mathcal{F}_t)_{t=1}^\infty$ is a *martingale difference sequence* if $\mathbb{E}[|D_t|] < \infty$ and $\mathbb{E}[D_t | \mathcal{F}_{t-1}] = 0$ for each t .

If $(X_t)_{t=1}^\infty$ is a *nonnegative supermartingale* with respect to $(\mathcal{F}_t)_{t=1}^\infty$ and $X_1 = 1$, then Ville’s inequality (Ville, 1939) states that, for any $\alpha \in (0, 1)$,

$$\mathbb{P}(\exists t \geq 1 : X_t > 1/\alpha) \leq \alpha. \quad (2.1)$$

Ville’s inequality is the primary tool for constructing confidence sequences, as illustrated in, e.g., Howard et al. (2021); in fact, it is the only admissible way to construct them (Ramdas et al., 2020). Given $\alpha \in (0, 1)$, a $(1 - \alpha)$ -level *confidence sequence (CS)* for a time-varying sequence of target parameters $(\theta_t)_{t=1}^\infty$ is a sequence of confidence intervals (CIs) $(C_t)_{t=1}^\infty$ such that

$$\mathbb{P}(\exists t \geq 1 : \theta_t \notin C_t) \leq \alpha, \text{ or equivalently, } \mathbb{P}(\forall t \geq 1 : \theta_t \in C_t) \geq 1 - \alpha. \quad (2.2)$$

This coverage guarantee over all times is sometimes referred to as being *time-uniform* or *anytime-valid*. In particular, the guarantee remains valid at arbitrary stopping times and without a pre-specified sample size, so that collecting additional data over time does not

invalidate it. This is a crucial difference of a CS from a fixed-time CI C_n , which only satisfies the following (much) weaker condition:

$$\forall n \geq 1, \mathbb{P}(\theta_n \notin C_n) \leq \alpha, \text{ or equivalently, } \forall n \geq 1, \mathbb{P}(\theta_n \in C_n) \geq 1 - \alpha. \quad (2.3)$$

2.2 Proper Scoring Rules

Given a probability forecast $p \in [0, 1]$ for the binary outcome y , whose (unknown) mean is $r \in [0, 1]$, we define *scoring rule*⁴ $S : [0, 1] \times [0, 1] \rightarrow \mathbb{R}$ as any function that quantifies the quality of the forecast p compared against r (or y , when r is unknown). Following [Gneiting and Raftery \(2007\)](#), we take scoring rules to be *positively oriented*, in the sense that larger scores indicate better forecasts.

A scoring rule is *proper* if $S(r, r) \geq S(p, r)$ for any $p, r \in [0, 1]$, and it is *strictly proper* when $S(r, r) = S(p, r)$ if and only if $p = r$. Proper scoring rules are typically considered as the primary means of evaluating probabilistic forecasts, as they encourage forecasters to be honest ([Garthwaite et al., 2005](#)), in the sense that they have no reason to report forecasts that are more optimistic/pessimistic than their actual beliefs about the eventual outcome.

Classical examples of proper scoring rules for binary outcomes include the following:

- The Brier score or the quadratic score ([Brier, 1950](#)):

$$S(p, r) = -(p - r)^2.$$

- The spherical score ([Good, 1971](#)):

$$S(p, r) = \frac{pr + (1 - p)(1 - r)}{\sqrt{p^2 + (1 - p)^2}}.$$

- The logarithmic score ([Good, 1952](#)):

$$S(p, r) = r \log(p) + (1 - r) \log(1 - p).$$

- The zero-one score or the success rate:

$$S(p, r) = r \mathbf{1}(p \geq 0.5) + (1 - r) \mathbf{1}(p < 0.5).$$

The Brier, spherical, and logarithmic scores are examples of strictly proper scoring rules, while the zero-one score is an example of a proper but not strictly proper scoring rule. It is important to note that, when comparing two forecasts p and q against r , we have that $S(p, r) - S(q, r)$ is linear in r for all of these examples. Also note that all of the examples except the logarithmic score are bounded for $p, r \in [0, 1]$.

⁴The literature on scoring rules is extensive and encompasses forecasts in the form of general probability distributions. We start our discussion with probability forecasts on binary outcomes, and then discuss the cases of categorical, vector-valued, and continuous outcomes in Section 4. See, e.g., [Winkler et al. \(1996\)](#); [Gneiting and Raftery \(2007\)](#); [Gneiting et al. \(2007\)](#) for a more comprehensive overview.

3 Confidence Sequences for Forecast Score Differentials

In this section, we derive confidence sequences for the time-varying difference in the quality of forecasts, as measured by a proper scoring rule. Our intuition comes from the extensive literature on evaluating and comparing probability forecasts via scoring rules (Winkler et al., 1996; Gneiting and Raftery, 2007; DeGroot and Fienberg, 1983; Schervish, 1989; Lai et al., 2011), combined with the powerful tool of time-uniform confidence sequences (Darling and Robbins, 1967; Howard et al., 2021).

3.1 A Game-Theoretic Motivation

The intuition behind our CS for forecast score differentials comes from the game-theoretic statistical framework (Shafer and Vovk, 2019). Consider a forecasting game where two players make probability forecasts on an event that happens over time (e.g., whether it will rain on each day, whether a sports team will win its game each week, and more) and an unknown player named reality generates the sequence of binary outcomes that the forecasters are trying to predict. Let $t \geq 1$ denote each round of the game and $y_{-(H-1)}, \dots, y_{-1}, y_0$ be the outcome of the event in the past H rounds. (Having any historical data is allowed but also not required by our framework, i.e., H could be any nonnegative integer including zero.) Then, the game can be formulated as follows:

Game 3.1 (Sequentially Comparing Forecasts on Binary Outcomes). *For rounds $t = 1, 2, \dots$:*

1. *Forecaster 1 makes their probability forecast, $p_t \in [0, 1]$.*
2. *Simultaneously, Forecaster 2 makes their probability forecast, $q_t \in [0, 1]$.*
3. *Reality chooses $r_t \in [0, 1]$. Note that r_t is not revealed to the forecasters.*
4. *$y_t \sim \text{Ber}(r_t)$ is sampled and revealed to the forecasters.*

At each round t , forecasters can make their probability forecasts using any information available to them, including historical and previous outcomes $y_{-(H-1)}, \dots, y_0, y_1, \dots, y_{t-1}$, any of the previous forecasts made, $p_1, \dots, p_{t-1}, q_1, \dots, q_{t-1}$, as well as any other external information available to them. They cannot, however, make predictions based on any of the r_t 's as well as information from the future.

There are several important benefits to deriving a valid sequential inference approach for comparing the two forecasters over time in Game 3.1. First, there are no assumptions of stationarity or conditional independence on the sequence $(r_t)_{t=1}^\infty$ that generates the binary outcomes $(y_t)_{t=1}^\infty$, meaning that the approach would be valid for *any* sequence of binary outcomes. Also, there are no assumptions made on how the individual forecasts $(p_t)_{t=1}^\infty$ and $(q_t)_{t=1}^\infty$ are made, other than the fact that they do not depend on the unknown sequence $(r_t)_{t=1}^\infty$ that generates the outcomes $(y_t)_{t=1}^\infty$. Finally, the game is naturally sequential, such that the most useful comparison of the two forecasters would be to consider their performance over time. In particular, the comparison should be valid *at any given time*, as opposed to having a fixed sample size, and reflect which one is *usually*, as opposed to absolutely or always, better. The CSs we derive in the forthcoming sections will take advantage of all of these benefits, contrasting with existing approaches that fall short on one or more of these aspects.

3.2 The Formal Setup

We now formalize Game 3.1 in the context of comparing the two probability forecasters over time. Let $(p_t)_{t=1}^\infty$ and $(q_t)_{t=1}^\infty$ be any pair of sequences of probability forecasts, each taking a value in $[0, 1]$, for a sequence of binary outcomes $(y_t)_{t=1}^\infty$. (We discuss extensions to bounded real-valued outcomes and vector-valued outcomes in a later section.) As illustrated in Game 3.1, the forecast p_t or q_t at time t can depend on *any* available information before observing y_t , including previous outcomes $y_{-H}, \dots, y_0, y_1, \dots, y_{t-1}$, (own or others') forecasts $p_1, \dots, p_{t-1}, q_1, \dots, q_{t-1}$, as well as any other external information.

Forecasters' filtration $(\mathcal{G}_t)_{t=1}^\infty$. We represent any information available to the forecasters before making their predictions at time t collectively as \mathcal{G}_{t-1} — in other words, $(\mathcal{G}_t)_{t=1}^\infty$ is a filtration to which $(p_t)_{t=1}^\infty$ and $(q_t)_{t=1}^\infty$ are predictable. Note that the framework allows for k -step ahead forecasts $(p_{t+k})_{t=1}^\infty$ and $(q_{t+k})_{t=1}^\infty$ for any $k \geq 1$, which are also predictable w.r.t. $(\mathcal{G}_t)_{t=1}^\infty$. Aside from requiring that the forecasts cannot depend on the future, we put no restrictions on how these forecasts are generated (Dawid, 1984).

Reality's filtration $(\mathcal{F}_t)_{t=1}^\infty$. Now suppose, without the loss of generality, that the sequence of binary outcomes $(y_t)_{t=1}^\infty$ generated by $y_t \sim \text{Ber}(r_t)$, for an unknown probability sequence $(r_t)_{t=1}^\infty$ with $r_t \in [0, 1]$. Importantly, we place no distributional assumptions on $(r_t)_{t=1}^\infty$, including stationarity or independence, so the formulation is completely general. We even allow r_t to be chosen adversarially, in the sense that the reality is chosen after the forecasts p_t and q_t are made. Hence, we denote \mathcal{F}_{t-1} as all accumulated information before the binary outcome y_t is realized, such that $\mathcal{F}_t \supset \mathcal{G}_t$ and $r_t \in \mathcal{F}_{t-1}$ for each t . Note that $(p_t)_{t=1}^\infty$, $(q_t)_{t=1}^\infty$, and $(r_t)_{t=1}^\infty$ are predictable w.r.t. $(\mathcal{F}_t)_{t=1}^\infty$. Using this notation, we arrive at the following key condition:

$$\mathbb{E}[y_t \mid \mathcal{F}_{t-1}] = r_t. \quad (3.1)$$

That is, r_t is the mean of y_t conditional on the reality's filtration \mathcal{F}_{t-1} , for each t .

Now, given a pair of probability forecasts, we can use scoring rules to assess compare their quality. Following the formulation by Lai et al. (2011), we define the **average (forecast) score differential** Δ_t between the sequences of forecasts $(p_i)_{i=1}^\infty$ and $(q_i)_{i=1}^\infty$, up to time t , as follows:

$$\Delta_t := \frac{1}{t} \sum_{i=1}^t [S(p_i, r_i) - S(q_i, r_i)]. \quad (3.2)$$

The time-varying parameter Δ_t provides an intuitive way of quantifying the difference in the quality of forecasts made up to time t . It is important to note that Δ_t quantifies how much one forecaster is better than the other *on average* (of time), as opposed to one strictly dominating the other (Giacomini and White, 2006; Henzi and Ziegel, 2021). We also note that, if S is bounded, e.g., when it is the Brier score, then $S(p, r) - S(q, r)$ is also bounded for any $p, q, r \in [0, 1]$.

Note that Δ_t is not observable to the forecasters or statistician, because reality's moves r_1, \dots, r_t are unknown and never observed. We thus define the **empirical average (forecast) score differential** $\hat{\Delta}_t$ using the actual outcomes y_1, \dots, y_t instead:

$$\hat{\Delta}_t := \frac{1}{t} \sum_{i=1}^t [S(p_i, y_i) - S(q_i, y_i)]. \quad (3.3)$$

Our goal as the statistician then becomes quantifying how far $\hat{\Delta}_t$ is from Δ_t , while accounting for uncertainty associated with sampling y_t at each time t . To achieve this goal, we define the *pointwise (forecast) score differential* $\delta_i := S(p_i, r_i) - S(q_i, r_i)$ as well as its empirical counterpart $\hat{\delta}_i := S(p_i, y_i) - S(q_i, r_i)$. In the following sections, we establish conditions with which the difference sequence $(\hat{\delta}_i - \delta_i)_{i=1}^\infty$ forms a martingale difference sequence (MDS), such that their cumulative sums $t(\hat{\Delta}_t - \Delta_t)$ can be uniformly bounded via a nonnegative supermartingale. As a result, we will be able to estimate and cover Δ_t using confidence sequences that only depend on observable quantities.

3.3 Scoring Rules with Linear Equivalentents

The key condition to deriving a valid CS for comparing forecasters is to consider scoring rules with linear equivalentents. Following Lai et al. (2011), we say that a scoring rule S has a *linear equivalent* \tilde{S} if, for any p and r , $\tilde{S}(p, r)$ is a linear function of r and $S(p, r) - \tilde{S}(p, r)$ does not depend on p . For example, the Brier score $S(p, r) = -(p - r)^2$ has a linear equivalent $\tilde{S}(p, r) = 2pr - p^2$.⁵ Also, any scoring rule S that is already linear in r , such as the spherical score and the zero-one score, trivially has a linear equivalent ($\tilde{S} = S$). By definition, if a scoring rule has a linear equivalent, then we can compute the difference in scores between two forecasters only using the linear equivalentents.

Scoring rules with linear equivalentents satisfy the key condition for our forthcoming CSs.

Lemma 3.1 (Lai et al. (2011)). *If S has a linear equivalent, then for each $i \geq 1$,*

$$\mathbb{E} \left[\hat{\delta}_i \mid \mathcal{F}_{i-1} \right] = \delta_i. \quad (3.4)$$

The proof, provided in Appendix B.1, is a simple application of the definition of linear equivalentents and the linearity of expectation. To be clear, the condition (3.4) essentially implies that the sequence $(\hat{\delta}_i - \delta_i)_{i=1}^\infty$ forms a martingale difference sequence w.r.t. $(\mathcal{F}_t)_{t=1}^\infty$. Lai et al. (2011) established this fact and used the martingale central limit theorem to obtain asymptotic CIs for Δ_n with fixed sample size n . Building upon this result, we now apply time-uniform bounds using nonnegative supermartingales to obtain anytime-valid and non-asymptotic CSs, which we describe in the next section.

3.4 Time-Uniform Confidence Sequences for Δ_t

3.4.1 Time-uniform Boundaries and Exponential Supermartingales

Given a scoring rule with a linear equivalent, we now show that we can uniformly bound the difference between $\hat{\Delta}_t$ and Δ_t over time using uniform boundaries and nonnegative supermartingales. To do this, we first define the *cumulative sum* $S_t := \sum_{i=1}^t (\hat{\delta}_i - \delta_i)$ as well as its *intrinsic time* \hat{V}_t , which represents an estimate of the variance process for the cumulative sum S_t . Our goal is then to uniformly bound the sum S_t over the intrinsic time \hat{V}_t , which corresponds to bounding the difference between $\hat{\Delta}_t$ and Δ_t over time, as $\hat{\Delta}_t - \Delta_t = \frac{1}{t} \sum_{i=1}^t (\hat{\delta}_i - \delta_i) = S_t/t$. Note that $(S_t)_{t=1}^\infty$ and $(\hat{V}_t)_{t=1}^\infty$ are adapted to $(\mathcal{F}_t)_{t=1}^\infty$.

Given the sums $(S_t)_{t=1}^\infty$ and their intrinsic times $(\hat{V}_t)_{t=1}^\infty$, we define a *uniform boundary* $u = u_\alpha$ as any function of the intrinsic times that gives a time-uniform bound on the sums:

⁵The logarithmic scoring rule $S(p, r) = r \log p + (1 - r) \log(1 - p)$ can also be viewed as a linear equivalent of the (negative) Kullback-Leibler divergence $S_{\text{KL}}(p, r) = -r \log \frac{r}{p} - (1 - r) \log \frac{1-r}{1-p}$. We focus on the Brier score in our subsequent analysis, however, because the logarithmic score is unbounded.

for any $\alpha \in (0, 1)$,

$$\mathbb{P}\left(\forall t \geq 1 : S_t \leq u_\alpha(\hat{V}_t)\right) \geq 1 - \alpha, \quad (3.5)$$

i.e., with high probability, the sums S_t are upper-bounded by $u(\hat{V}_t)$ at all times t . By applying the same uniform boundary to $-S_t$, we can also obtain a time-uniform lower bound on S_t . We defer a more formal definition of uniform boundaries in Appendix A.

How do we show that there exists such a uniform boundary for our definitions of S_t and \hat{V}_t ? Howard et al. (2020, 2021) show that there exists a uniform boundary for (S_t, \hat{V}_t) if

$$L_t(\lambda) = \exp\left\{\lambda S_t - \psi(\lambda)\hat{V}_t\right\} \quad (3.6)$$

is a supermartingale for each $\lambda \in [0, \lambda_{\max})$, where $\psi : [0, \lambda_{\max}) \rightarrow \mathbb{R}$ is a cumulant generative function (CGF) of a random variable, such as the Gaussian CGF $\psi_N(\lambda) = \frac{\lambda^2}{2}$, the exponential CGF $\psi_{E,c}(\lambda) = c^{-2}(-\log(1 - c\lambda) - c\lambda)$, and the gamma CGF $\psi_{G,c}(\lambda) = \frac{\lambda^2}{2(1-c\lambda)}$. The uniform boundary u for a CGF ψ in this construction is also called a *sub- ψ uniform boundary* (or sub-Gaussian, sub-exponential, and sub-gamma uniform boundaries if the CGF corresponds to a Gaussian, exponential, and gamma respectively).

Our goal is now to identify the conditions in which $L_t(\lambda)$ is indeed a supermartingale and use different CGFs to obtain different uniform boundaries and hence CSs. The resulting CSs all lead to an anytime-valid sequential inference procedure for Δ_t , with virtually no distributional assumptions on the outcomes or the forecasts.

3.4.2 Warmup: Hoeffding-Style Confidence Sequences for Δ_t

We first derive an illustrative example of a CS for Δ_t solely based on the sub-Gaussianity of the pointwise score differentials $(\hat{\delta}_i)_{i=1}^\infty$. While the resulting CS is not the tightest one in our case, its derivation is simple enough to showcase the general pipeline for deriving CSs.

Recall the problem setup in Section 3.2. For each $i \geq 1$, given that the probability forecasts $p_i, q_i \in [0, 1]$ as well as the binary outcome $y_i \in \{0, 1\}$ and its unknown mean $r_i \in [0, 1]$ are all bounded, we know that the pointwise score differentials $\hat{\delta}_i$ and δ_i are bounded (between -1 and 1 , specifically) for many of the scoring rules we've discussed (e.g., the Brier score, the spherical score, and the zero-one score). This implies that, assuming (3.4), we have that $\hat{\delta}_i$ is 1-sub-Gaussian⁶ conditioned on \mathcal{F}_{i-1} , meaning that $\mathbb{E}[e^{\lambda(\hat{\delta}_i - \delta_i)} \mid \mathcal{F}_{i-1}] \leq e^{\lambda^2/2}$ for all $\lambda \in \mathbb{R}$, or equivalently,

$$\mathbb{E}\left[\exp\left\{\lambda\left(\hat{\delta}_i - \delta_i\right) - \psi_N(\lambda)\right\} \mid \mathcal{F}_{i-1}\right] \leq 1, \quad \forall \lambda \in \mathbb{R}, \quad (3.7)$$

where $\psi_N(\lambda) = \frac{\lambda^2}{2}$ is the Gaussian CGF.

Now, assuming $|\hat{\delta}_i| \leq 1$ for each i , and simply define the intrinsic time as $\hat{V}_t = \sum_{i=1}^t 1 = t$. It then follows that, for each $\lambda \in [0, \infty)$, the exponential process $L_t(\lambda) = \exp\{\lambda S_t - \psi_N(\lambda)\hat{V}_t\}$ is a supermartingale:

$$\mathbb{E}[L_t(\lambda) \mid \mathcal{F}_{t-1}] = L_{t-1}(\lambda) \cdot \mathbb{E}\left[\exp\left\{\lambda\left(\hat{\delta}_t - \delta_t\right) - \psi_N(\lambda) \cdot 1\right\} \mid \mathcal{F}_{t-1}\right] \leq L_{t-1}(\lambda). \quad (3.8)$$

Hence, there exists a sub-Gaussian uniform boundary for (S_t, \hat{V}_t) such that (3.5) holds. We summarize the result in the following theorem. We use the notation $(a \pm b)$ to denote the confidence interval $(a - b, a + b)$.

⁶See, e.g., Example 2.4 as well as Exercise 2.4 in Wainwright (2019).

Theorem 3.1 (Hoeffding-Style Confidence Sequences for Δ_t). *Suppose that $\mathbb{E}[\hat{\delta}_i | \mathcal{F}_{i-1}] = \delta_i$ and $|\hat{\delta}_i| \leq 1$ for each $i \geq 1$. Then, for any $\alpha \in (0, 1)$,*

$$C_t^{\text{H}} := \left(\hat{\Delta}_t \pm \frac{u(t)}{t} \right) \quad \text{forms a } (1 - \alpha)\text{-CS for } \Delta_t, \quad (3.9)$$

where $u = u_{\alpha/2}$ is any sub-Gaussian uniform boundary with crossing probability $\alpha/2$.

The statement (3.9) is equivalent to saying that, with probability at least $1 - \alpha$, Δ_t is contained in C_t^{H} for all time t , or that $\mathbb{P}(\forall t \geq 1 : \Delta_t \in C_t^{\text{H}}) \geq 1 - \alpha$. This CS is called a Hoeffding-style CS, as it extends Hoeffding’s inequality for the sums of independent sub-Gaussian random variables (Hoeffding, 1963) to the sequential case. Note that the conditions are satisfied when using scoring rules that have linear equivalents (Lemma 3.1) and are bounded on $[0, 1] \times [0, 1]$, including the Brier score, the spherical score, and the zero-one score. For the unbounded logarithmic score, one can use its truncated variant $S(p, r) = r \log(p \vee \epsilon) + (1 - r) \log(1 - (p \vee \epsilon))$ for some small $\epsilon > 0$, although the score is no longer proper. As for the choice of the sub-Gaussian uniform boundary u , we defer our discussion to Section 3.4.4.

3.4.3 Main Result: Empirical Bernstein Confidence Sequences for Δ_t

Now we are ready to present our main result, which is the derivation of a tight CS for Δ_t . The key difference from the Hoeffding-style CS is that we now use an empirical estimate of the variance process for the cumulative sums, leading to an empirical Bernstein (EB) CS.⁷

Recall the problem setup in Section 3.2 once again.

Theorem 3.2 (Empirical Bernstein Confidence Sequences for Δ_t). *Suppose that $\mathbb{E}[\hat{\delta}_i | \mathcal{F}_{i-1}] = \delta_i$ and $|\hat{\delta}_i| \leq \frac{c}{2} < \infty$ for each $i \geq 1$. Also, let $\hat{V}_t = \sum_{i=1}^t (\hat{\delta}_i - \gamma_i)^2$, where $(\gamma_i)_{i=1}^{\infty}$ is any $[-\frac{c}{2}, \frac{c}{2}]$ -valued predictable sequence w.r.t. $(\mathcal{F}_i)_{i=1}^{\infty}$. Then, for any $\alpha \in (0, 1)$,*

$$C_t^{\text{EB}} := \left(\hat{\Delta}_t \pm \frac{u(\hat{V}_t)}{t} \right) \quad \text{forms a } (1 - \alpha)\text{-CS for } \Delta_t, \quad (3.10)$$

where $u = u_{\alpha/2, c}$ is any sub-exponential uniform boundary with crossing probability $\alpha/2$ and scale c .

As before, the statement (3.10) is equivalent to saying that, with probability at least $1 - \alpha$, Δ_t is contained in C_t^{EB} for all time t , or that $\mathbb{P}(\forall t \geq 1 : \Delta_t \in C_t^{\text{EB}}) \geq 1 - \alpha$. The proof is provided in Appendix B.2. Theorem 3.2 (and its proof) can be viewed as an extension of Theorem 4 in Howard et al. (2021) to our setup of sequential forecast comparison.

We highlight that Theorem 3.2 matches all the desiderata described in Section 3.1. Notably, it holds for virtually *any* sequence of probability forecasts and for *any* sequence of outcomes, without any stationarity or conditional independence assumptions on the outcomes (“distribution-free”), and it remains true even when the outcomes are chosen adversarially after the forecasts are already made. There are also no assumptions on the forecasts, as long as they are made without already knowing the outcome (which cannot happen in realistic forecasting tasks). Our confidence sequences therefore provide a virtually assumption-free sequential inference procedure for comparing probability forecasters over time.

⁷The improvement from a Hoeffding-style CS to an empirical Bernstein CS mirrors the improvement from Hoeffding’s inequality for independent sub-Gaussian random variables to empirical Bernstein’s inequality for independent sub-exponential random variables in the fixed-sample case. Also note that sub-Gaussian random variables are sub-exponential. See, e.g., Section 2.1 of Wainwright (2019), for a review.

Type	CS C_t	Intrinsic Time \hat{V}_t	Uniform Boundary u
Hoeffding-Style (Theorem 3.1)	$\left(\hat{\Delta}_t \pm \frac{u(\hat{V}_t)}{t}\right)$	t	Polynomial Stitching Normal Mixture
Emp. Bernstein (Theorem 3.2)	$\left(\hat{\Delta}_t \pm \frac{u(\hat{V}_t)}{t}\right)$	$\sum_{i=1}^t (\hat{\delta}_i - \gamma_i)^2$, $(\gamma_i)_{i=1}^\infty$ predictable	Polynomial Stitching Gamma-Exponential Mixture

Table 3: Summary of confidence sequences and their uniform boundary choices.

As in Theorem 3.1, Lemma 3.1 gives the first condition for Theorem 3.2, meaning that we can use any bounded scoring rule with linear equivalents, including the Brier score, the spherical score, and the zero-one score (proper), as well as the truncated logarithmic score (improper). We will also show in Section 4.4 that a normalized version of the score can be used.

A reasonable choice for the predictable sequence $(\gamma_i)_{i=1}^\infty$ is the average of previous score differentials, i.e., $\gamma_i = \hat{\Delta}_{i-1}$, although a smarter choice may lead to tighter CS. We use $\gamma_i = \hat{\Delta}_{i-1}$ throughout our experiments in this paper. The choice of the uniform boundary u is discussed in the following subsection.

For the rest of this paper, our default choice of CS for Δ_t will be that of Theorem 3.2, using $\hat{V}_t = \sum_{i=1}^t (\hat{\delta}_i - \hat{\Delta}_{i-1})^2$, unless specified otherwise.

3.4.4 Choosing the Uniform Boundary u

The specific choice of the uniform boundary u controls the tightness of the CS across time, and the extensive list of choices for u is covered in detail in Howard et al. (2021). While the simplest uniform boundaries are given as a linear function of the intrinsic time, curved uniform boundaries can produce CSs that are tighter across time. Here, we focus on two curved boundaries, applicable to both Theorems 3.1 and 3.2: the *polynomial stitching boundary* and the *conjugate-mixture (CM) boundary*.

First, the polynomial stitched boundary provides a closed-form bound on the difference in estimated and actual forecast score differentials. It is constructed by finding a smooth analytical upper bound on a sequence of linear uniform bounds across different timesteps. The polynomial stitched boundary, which we denote as $u_\alpha^S(v)$, asymptotically grows with $O(\sqrt{v \log \log v})$ rate, matching the form of the law of the iterated logarithm (LIL). For example, the 95% CS for Δ_t is given as follows (assuming $|\hat{\delta}_t - \delta_t| \leq 2$ for all $t \geq 1$):

$$\hat{\Delta}_t \pm 2 \cdot \frac{1.7 \sqrt{\left(\hat{V}_t \vee 1\right) \left(\log \log \left(2 \left(\hat{V}_t \vee 1\right)\right) + 3.8\right) + 3.4 \log \log \left(2 \left(\hat{V}_t \vee 1\right)\right) + 13}{t} \quad (3.11)$$

where \hat{V}_t is the intrinsic time and $a \vee b = \max\{a, b\}$. Note that the width of the CS, given by $\frac{2}{t} u_{\alpha/2}^S(\hat{V}_t)$, shrinks toward zero at a $O(1/\sqrt{t})$ rate up to logarithmic factors, which is characteristic of CSs based on uniform boundaries.

The polynomial stitched boundary can be applied to both Theorems 3.1 and 3.2 by setting $\hat{\Delta}_t = t$ and $\hat{V}_t = \sum_{i=1}^t (\hat{\delta}_i - \gamma_i)^2$ respectively: previous work has shown that the polynomial stitched boundary is a sub-gamma uniform boundary (Theorem 1, Howard et al. (2021)), and also that a sub-gamma uniform boundary is also a sub-Gaussian and a sub-exponential uniform boundary (Proposition 1, Howard et al. (2020)).

The second choice of u , which is our default choice in our subsequent experiments, is the CM boundary. The CM boundary represents a class of uniform boundaries arising from the following lemma:

Lemma 3.2 (Lemma 2, Howard et al. (2021)). *Given a CGF $\psi : [0, \lambda_{\max}) \rightarrow [0, \infty)$, a probability distribution F on $[0, \lambda_{\max})$, and $\alpha \in (0, 1)$,*

$$u_{\alpha}^{\text{CM}}(v; \psi) := \sup \left\{ s \in \mathbb{R} : \underbrace{\int \exp \{ \lambda s - \psi(\lambda) v \} dF(\lambda)}_{=: m(s, v)} < \frac{1}{\alpha} \right\} \quad (3.12)$$

is a sub- ψ uniform boundary with crossing probability α , so long as the supermartingale $(L_t(\lambda))_{t=1}^{\infty}$ in (3.6) is product measurable with respect to $(\mathcal{F}_t)_{t=1}^{\infty}$ and the independent random variable λ .

The term $\exp\{\lambda s - \psi(\lambda)v\}$ inside the integral in (3.12) can be viewed as the supermartingale $L_t(\lambda)$ in (3.6), and given a specific choice of ψ (e.g., Gaussian and exponential) it can be shown that one can choose F as the conjugate distribution (e.g., Gaussian and gamma) to evaluate the integral $m(s, v)$ in closed-form.

In the case where ψ is the Gaussian CGF, corresponding to the Hoeffding-style CS in Theorem 3.1, the sub-Gaussian CM boundary itself can also be computed in closed-form:

$$u_{\alpha}^{\text{CM}}(v; \psi_N) = \sqrt{(v + \rho) \log \left(\frac{v + \rho}{\alpha^2 \rho} \right)} \quad (3.13)$$

where $\rho > 0$ is a hyperparameter that controls the intrinsic time at which the bound can be its tightest. This boundary corresponds to the classical *normal mixture* by Robbins (1970).

In the case of the exponential CGF, corresponding to the empirical Bernstein CS in Theorem 3.2, the sub-exponential CM boundary $u_{\alpha}^{\text{CM}}(v; \psi_E)$ does not have a closed form (the integral $m(s, v)$ has a closed form; the boundary $u_{\alpha}^{\text{CM}}(v; \psi_E)$ does not), although in practice it can still be computed efficiently using a numerical root finder. As the sub-exponential CM boundary uses the gamma-exponential conjugacy, we also refer to it as the *gamma-exponential mixture* uniform boundary. Also, while the CM boundary has an asymptotic rate of $O(\sqrt{v \log v})$ as illustrated in (3.13), it is usually tighter than the polynomial stitched boundary in practice. In fact, the CM boundary is shown to be unimprovable in the case of sub-Gaussian random variables unless more assumptions are made (Proposition 4, Howard et al. (2021)).

Table 3 summarizes the choice of uniform boundaries and the CSs we derived for estimating Δ_t . In our experiments, we mostly use the appropriate CM boundary, although we also perform an empirical comparison between the different choices as well as their hyperparameters in Appendix D. Finally, we note that we use the publicly available implementation of the polynomial stitching and CM uniform boundaries by Howard et al. (2021).⁸

3.5 e-Processes and Anytime-Valid p-Processes

While our derivation so far has focused on confidence sequences, we can also derive e-processes and anytime-valid p-processes (Shafer and Vovk, 2019; Vovk and Wang, 2021; Grünwald et al., 2019; Ramdas et al., 2020), using the exponential supermartingale (3.6) that we used to

⁸<https://github.com/gostevhoward/confseq>

construct the CS in the previous section. This correspondence is general to any exponential process upper-bounded by a NSM, as noted in, e.g., [Ramdas et al. \(2020\)](#); [Howard et al. \(2021\)](#). For the sake of exposition, we illustrate this correspondence in the case of the CS derived in [Theorem 3.2](#).

Weak and Strong Null Hypotheses. Before deriving e- and p-processes, we must first make clear the null hypotheses that correspond to the CS derived in [Theorem 3.2](#). We define the *weak one-sided null* $H_0^w(p, q)$ as

$$H_0^w(p, q) : \Delta_t = \frac{1}{t} \sum_{i=1}^t \delta_i = \frac{1}{t} \sum_{i=1}^t \mathbb{E} \left[\hat{\delta}_i \mid \mathcal{F}_{i-1} \right] \leq 0. \quad (3.14)$$

$H_0^w(p, q)$ corresponds to saying that the first forecaster (p) is no better than the second forecaster (q) *on average* up to a non-pre-specified time t . $H_0^w(q, p)$ is analogously defined as $H_0^w(q, p) : -\Delta_t = -\frac{1}{t} \sum_{i=1}^t \delta_i \leq 0$.

Our confidence sequences derived in [Theorem 3.2](#) would correspond to sequential tests for both of the weak one-sided nulls $H_0^w(p, q)$ and $H_0^w(q, p)$, as they have a time-uniform coverage guarantee for the quantity Δ_t . Specifically, in the case of our CSs, a $(1 - \alpha)$ -level CS for Δ_t denoted as $C_t = (L_t, U_t)$ implies that $\Delta_t \leq U_t$ with probability at least $1 - \frac{\alpha}{2}$ and that $\Delta_t \geq L_t$ with probability at least $1 - \frac{\alpha}{2}$, so if for any time t we find that $L_t > 0$ or $U_t < 0$, then we can reject either $H_0^w(p, q)$ or $H_0^w(q, p)$ with high probability.

We also define the *strong one-sided null* $H_0^s = H_0^s(p, q)$ as

$$H_0^s(p, q) : \delta_i = \mathbb{E} \left[\hat{\delta}_i \mid \mathcal{F}_{i-1} \right] \leq 0 \quad \forall i = 1, \dots, t. \quad (3.15)$$

$H_0^s(q, p)$ is defined analogously as $H_0^s(q, p) : -\delta_i \leq 0 \forall i = 1, \dots, t$. In contrast to H_0^w , H_0^s corresponds to saying that the first forecaster (p) is no better than the second forecaster (q) *at every time step* $i = 1, \dots, t$. Thus, the strong null H_0^s implies the weak null H_0^w , but not vice versa. The critical distinction here is that rejecting $H_0^s(p, q)$ only tells us that the first forecaster outperformed the second one at some time step i , but it does not tell us if either was better over the rounds that we've observed. Notably, the recent work by [Henzi and Ziegel \(2021\)](#) provides sequential inference procedures for the strong one-sided null, contrasting with our approach that involves the weak version.

Note that, in a sequential setting where inference can be made for every time step t , the two-sided versions of H_0^w and H_0^s would coincide as the strong two-sided null, as both versions would imply that $\delta_i = 0 \forall i = 1, \dots, t$ when applied over time. Importantly, the sequential test implied by our CS from [Theorem 3.2](#) is *not* a test of the strong two-sided null but of two weak one-sided nulls, combined into one CS via a union bound.

e-Processes via Exponential Supermartingales. Having defined the null hypotheses, we can now show that the exponential supermartingale underlying the construction of our CSs in [Theorem 3.2](#) can be used to construct a sequence of random variables that measure the accumulated evidence against the weak one-sided null. Formally, an *e-process* ([Ramdas et al., 2021](#)) for the null H_0 is defined as a nonnegative sequence of random variables $(E_t)_{t=1}^\infty$, adapted to $(\mathcal{F}_t)_{t=1}^\infty$, such that under H_0 , the following holds:

$$\text{for any arbitrary stopping time } \tau, \quad \mathbb{E}_{H_0}[E_\tau] \leq 1, \quad (3.16)$$

where we take $E_\infty = \limsup_{t \rightarrow \infty} E_t$ for infinite stopping times. The term ‘process’ is used to emphasize the fact that the condition $\mathbb{E}_{H_0}[E_\tau] \leq 1$ is true under H_0 at arbitrary *stopping* times. Importantly, the time-uniform coverage guarantee for CSs is *equivalent* to coverage guarantees at arbitrary stopping times (Lemma 3, Howard et al. (2021); Proposition 1, Zhao et al. (2016)), such that our CSs derived for arbitrary (not necessarily stopping) times also have coverage guarantees at stopping times. For each t , E_t is also called an e-variable, and its realization is called an e-value (Vovk and Wang, 2021; Grünwald et al., 2019). The notion of measuring evidence against the null directly corresponds to increasing one’s wealth by betting against the null in game-theoretic statistics (Shafer, 2021).

We can now define and show an e-process that corresponds to Theorem 3.2. Recall once again the problem setup in Section 3.2.

Theorem 3.3 (Sub-exponential e-Processes for H_0^w). *Assume the same conditions as Theorem 3.2. Then, for each $\lambda \in [0, \lambda_{\max})$,*

$$E_t(\lambda) := \exp \left\{ \lambda \sum_{i=1}^t \hat{\delta}_i - \psi_{E,c}(\lambda) \hat{V}_t \right\} \quad \text{is an e-process for } H_0^w(p, q), \quad (3.17)$$

where $\psi_{E,c}$ is the sub-exponential CGF with scale c .

The proof, provided in Appendix B.3, shows that under H_0^w , $E_t(\lambda)$ is upper-bounded by the supermartingale analogous to $L_t(\lambda)$ in (3.6) now computed using $\lambda_1, \dots, \lambda_t$. For any choice of λ and any stopping time τ , $E_\tau(\lambda)$ provides a measure of accumulated evidence against the weak one-sided null $H_0^w(p, q)$, leading to an alternative sequential inference procedure for sequentially comparing forecasters in terms of their average performance over time. Also, note that for each t and $i = 1, \dots, t$, E_t can be calculated only using the forecasts p_i, q_i and the observed outcomes y_i , assuming γ_i is also computed using them (e.g., $\gamma_i = \hat{\Delta}_{i-1}$). Theorem 3.3 further allows us to directly compare our approach with Henzi and Ziegel (2021)’s e-processes for the strong one-sided null $H_0^s(p, q)$; we later provide an empirical comparison of the two procedures in Section 5.3.

Choosing λ for e-Processes. Choosing λ for $E_t(\lambda)$ in Theorem 3.3 is an easier task than choosing a uniform boundary u for C_t in Theorems 3.1 or 3.2, as it can be done within the first step of choosing a uniform boundary. This is because the first step of choosing a uniform boundary for a CS, as described in Section 3.4.4, corresponds to constructing the underlying supermartingale $L_t(\lambda)$ with the appropriate λ , which we can directly use for our e-processes.

For example, when using the CM boundary, which is our default choice, the integral $m(s, v)$ from (3.12) evaluated at $(\sum_{i=1}^t \hat{\delta}_i, \hat{V}_t)$ directly gives us the e-value at time t , where F is the conjugate distribution (Gaussian for Theorem 3.1; gamma for Theorem 3.2). Note that the integral $m(s, v)$ can be computed in closed-form for any CM boundaries, including the normal mixture and the gamma-exponential mixture⁹, even when the uniform boundary (3.12) cannot. The polynomial stitched bound also yields a form that corresponds to a discrete mixture (Theorem 2 in Howard et al. (2021)), such that a discrete sum (instead of an integral for CM) can be computed to give the e-value directly.

Anytime-Valid p-Processes. Finally, we also note that any e-process for H_0 can also be converted into an *anytime-valid p-process* for H_0 , which is defined as the sequence $(\mathbf{p}_t)_{t=1}^\infty$ that

⁹We derive the closed-form expression for the gamma-exponential mixture in Appendix C.

satisfies, for any $\alpha \in (0, 1)$:

$$\text{for any arbitrary stopping time } \tau, \quad \mathbb{P}_{H_0}(\mathbf{p}_\tau \leq \alpha) \leq \alpha. \quad (3.18)$$

Given an e-process $(E_t)_{t=1}^\infty$, we can convert it into an anytime-valid p-process via

$$\mathbf{p}_t := \inf_{i \leq t} 1/E_i. \quad (3.19)$$

following derivations from, e.g., [Ramdas et al. \(2020, 2021\)](#). \mathbf{p}_t can alternatively be defined from a CS as the smallest α for which the $(1 - \alpha)$ -level CS does not include zero ([Howard et al., 2021](#)), so all three notions (CS, e-values, and anytime-valid p-values) are closely related.

4 Extensions

In this section, we discuss a set of extensions that allow us to perform anytime-valid sequential forecast comparison beyond the case of probability forecasts on binary outcomes. While our derivation and experiments so far focused on the case of binary outcomes using the Brier score, [Theorem 3.1](#) and [Theorem 3.2](#) can be extended to other cases, some more readily than others. At a high level, the key is to consider other sequential forecasting scenarios where the condition [\(3.4\)](#) continues to hold.

4.1 Probabilistic Forecasts on Categorical Outcomes

So far, our derivation of a CS for the average forecast score differential Δ_t focused on the case of binary outcomes. We now show that essentially the same derivation can be done for comparing probabilistic forecasts made on categorical outcomes with K classes. As a result, we arrive at a time-uniform, non-asymptotic, and distribution-free sequential inference procedure for comparing two probabilistic forecasts on categorical outcomes without much additional work.

For each $t = 1, 2, \dots$, let $\mathbf{y}_t = (y_t^{(1)}, \dots, y_t^{(K)}) \in \{0, 1\}^K$ be the categorical outcome at time t represented as a one-hot vector (i.e., $\sum_{k=1}^K y_k = 1$). Let $\mathbf{p}_t = (p_t^{(1)}, \dots, p_t^{(K)}) \in \Delta^{K-1}$ and $\mathbf{q}_t = (q_t^{(1)}, \dots, q_t^{(K)}) \in \Delta^{K-1}$ be probabilistic forecasts made by two forecasters on \mathbf{y}_t , where Δ^{K-1} is the K -dimensional probability simplex (i.e., $p_t^{(k)} \in [0, 1]$ and $\sum_{k=1}^K p_t^{(k)} = 1$). Using these notations, we can set up an analogous game setup to [Game 3.1](#):

Game 4.1 (Sequentially Comparing Probabilistic Forecasts on Categorical Outcomes). *For rounds $t = 1, 2, \dots$:*

1. *Forecaster 1 makes their probabilistic forecast, $\mathbf{p}_t \in \Delta^{K-1}$.*
2. *Forecaster 2 makes their probabilistic forecast, $\mathbf{q}_t \in \Delta^{K-1}$.*
3. *Reality chooses $\mathbf{r}_t \in \Delta^{K-1}$. Note that \mathbf{r}_t is not revealed to the forecasters.*
4. *$\mathbf{y}_t \sim \text{Categorical}(\mathbf{r}_t)$ is sampled and revealed to the forecasters.*

At each round t , forecasters can make their probability forecasts using any information available to them, including historical and previous outcomes $\mathbf{y}_{-(H-1)}, \dots, \mathbf{y}_0, \mathbf{y}_1, \dots, \mathbf{y}_{t-1}$, any of the previous forecasts made, $\mathbf{p}_1, \dots, \mathbf{p}_{t-1}$, $\mathbf{q}_1, \dots, \mathbf{q}_{t-1}$, as well as any other external information available to them. They cannot, however, make predictions based on any of the \mathbf{r}_t 's as well as information from the future.

This game is equivalent to Game 3.1 when $K = 2$, as we can use the one-hot representation of the binary outcomes and set $\mathbf{p}_t := (1-p_t, p_t)$. The reality still plays the role of specifying the unknown mean of the outcomes by now specifying a K -categorical distribution. Generalizing the corresponding definitions of the forecasters' filtration $(\mathcal{G}_t)_{t=1}^\infty$ and the reality's filtration $(\mathcal{F}_t)_{t=1}^\infty$ from Section 3.2 to these forecasts, we have the following analog of (3.1):

$$\mathbb{E}[\mathbf{y}_t \mid \mathcal{F}_{t-1}] = \mathbf{r}_t \quad \forall t. \quad (4.1)$$

The classical examples of proper scoring rules for binary outcomes, as well as their key properties, also generalize seamlessly to the categorical case.

- The Brier score or the quadratic score (Brier, 1950):

$$S(\mathbf{p}, \mathbf{r}) = -\|\mathbf{p} - \mathbf{r}\|_2^2.$$

- The spherical score (Good, 1971):

$$S(\mathbf{p}, \mathbf{r}) = \frac{\mathbf{p}^T \mathbf{r}}{\|\mathbf{p}\|_2}.$$

- The logarithmic score (Good, 1952):

$$S(\mathbf{p}, \mathbf{r}) = \log(\mathbf{p})^T \mathbf{r}.$$

- The zero-one score or the success rate:

$$S(\mathbf{p}, \mathbf{r}) = \mathbf{1}(\mathbf{p} \geq 0.5)^T \mathbf{r}.$$

where we define vector-valued evaluations of basic arithmetic functions by their elementwise application, i.e., $\log(\mathbf{p}) := (\log p^{(k)})_{k=1}^K$ and $\mathbf{1}(\mathbf{p} \geq 0.5) := (\mathbf{1}(p^{(k)} \geq 0.5))_{k=1}^K$. The Brier score has a linear equivalent in the form $\tilde{S}(\mathbf{p}, \mathbf{r}) = -\mathbf{p}^T \mathbf{p} + 2\mathbf{p}^T \mathbf{r}$, and the spherical, logarithmic, and zero-one scores are already linear in \mathbf{r} .

Using these scoring rules, we can analogously define the average forecast score differential Δ_t between $(\mathbf{p}_i)_{i=1}^\infty$ and $(\mathbf{q}_i)_{i=1}^\infty$ up to time t as

$$\Delta_t := \frac{1}{t} \sum_{i=1}^t [S(\mathbf{p}_i, \mathbf{r}_i) - S(\mathbf{q}_i, \mathbf{r}_i)]. \quad (4.2)$$

as well as its empirical estimate

$$\hat{\Delta}_t := \frac{1}{t} \sum_{i=1}^t [S(\mathbf{p}_i, \mathbf{y}_i) - S(\mathbf{q}_i, \mathbf{y}_i)]. \quad (4.3)$$

The pointwise differentials are also defined analogously, i.e., $\delta_i = S(\mathbf{p}_i, \mathbf{r}_i) - S(\mathbf{q}_i, \mathbf{r}_i)$ and $\hat{\delta}_i = S(\mathbf{p}_i, \mathbf{y}_i) - S(\mathbf{q}_i, \mathbf{y}_i)$ for each $i \geq 1$.

Then, given the same definitions of the score differentials as well as the categorical analogs of scoring rules with linear equivalents, it is clear that Lemma 3.1 as well as Theorems 3.1 and 3.2 still hold, meaning that the same time-uniform sequential inference procedures can be used for probabilistic forecasts on categorical outcomes.

4.2 k -Step-Ahead Forecasts

In many forecasting scenarios, it is common for forecasters to make k -step-ahead forecasts for an eventual binary or categorical outcome. For example, meteorologists would make 7-day forecasts each day, such that there are a total of seven forecasts made for each outcome (one made seven days ago, six days ago, and so on). To compare the overall performance of these forecasters over time, we consider a weighted average of their forecast scores. Assuming that we use scoring rules with linear equivalents, our derivation from Section 3 can readily be extended to the overall comparison of k -step-ahead forecasters. For notational simplicity, we focus on the case where the outcomes are binary, although an analogous extension to categorical outcomes will continue to hold as in Section 4.1.

For each $k = 1, \dots, K$, let $p_t^{(k)}$ and $q_t^{(k)}$ denote the k -step ahead probability forecasts by two forecasters on the eventual outcome y_t . Note that the forecasts $p_t^{(k)}$ and $q_t^{(k)}$ are made at the beginning of round $t - k + 1$. Then, Game 3.1 can be extended to k -step-ahead forecasts as follows:

Game 4.2 (Sequentially Comparing k -Step-Ahead Forecasts on Binary Outcomes). *Fix $K \geq 1$. For rounds $t = 1, 2, \dots$:*

1. *Forecaster 1 makes their k -step ahead probability forecasts, $p_t^{(1)}, p_{t+1}^{(2)}, \dots, p_{t+K-1}^{(K)} \in [0, 1]$.*
2. *Forecaster 2 makes their k -step ahead probability forecasts, $q_t^{(1)}, q_{t+1}^{(2)}, \dots, q_{t+K-1}^{(K)} \in [0, 1]$.*
3. *Reality chooses $r_t \in [0, 1]$. Note that r_t is not revealed to the forecasters.*
4. *$y_t \sim \text{Ber}(r_t)$ is sampled and revealed to the forecasters.*

At each round t , forecasters can make their probability forecasts at round t using any information available to them, including historical and previous outcomes $y_{-(H-1)}, \dots, y_0, y_1, \dots, y_{t-1}$, any of the previous forecasts made, as well as any other external information available to them. They cannot, however, make predictions based on any of the r_t 's as well as information from the future.

Given a scoring rule S with a linear equivalent \tilde{S} , along with pre-determined weights $\mathbf{w} = (w_1, \dots, w_K) \in [0, 1]^K$ such that $\sum_{k=1}^K w_k = 1$, we can define the weighted average of the previous k -step forecast scores as the measure of overall performance as follows. Let $\mathbf{p}_t = (p_t^{(1)}, p_t^{(2)}, \dots, p_t^{(K)})$ be the vector containing the K most recent probability forecasts made by a forecaster on the outcome y_t with mean r_t , sorted from the most recent to the least. Then, define

$$S_{\mathbf{w}}(\mathbf{p}_t, r_t) := \sum_{k=1}^K w_k S(p_t^{(k)}, r_t). \quad (4.4)$$

The scoring rule $S_{\mathbf{w}}$ now measures the overall quality of k -step ahead forecasts for $k = 1, \dots, K$, averaged using weights \mathbf{w} .¹⁰ Given two sequences of k -step-ahead forecasts, $(\mathbf{p}_t)_{t=1}^{\infty}$ and $(\mathbf{q}_t)_{t=1}^{\infty}$, we can compare them by analogously constructing a CS for their average forecast score differentials $(\Delta_t)_{t=1}^{\infty}$, now using $S_{\mathbf{w}}$:

$$\Delta_t = \frac{1}{t} \sum_{i=1}^t [S_{\mathbf{w}}(\mathbf{p}_i, r_i) - S_{\mathbf{w}}(\mathbf{q}_i, r_i)]. \quad (4.5)$$

¹⁰One can also verify that if S is proper, then $S_{\mathbf{w}}$ is also proper for $\mathbf{w} \in (0, 1)^K$, where we extend the definition of propriety to allow for vector-valued forecasts $\mathbf{p} \in [0, 1]^K$ in the first argument.

The empirical estimate is analogously defined as:

$$\hat{\Delta}_t = \frac{1}{t} \sum_{i=1}^t [S_{\mathbf{w}}(\mathbf{p}_i, y_i) - S_{\mathbf{w}}(\mathbf{q}_i, y_i)]. \quad (4.6)$$

With this definition of k -step-ahead forecasts and the scoring rule $S_{\mathbf{w}}$, we can derive an analog of Lemma 3.1, which then allows us to use the CS in Theorem 3.2.

Lemma 4.1. *Assume that S has a linear equivalent, and define $\delta_i = S_{\mathbf{w}}(\mathbf{p}_i, r_i) - S_{\mathbf{w}}(\mathbf{q}_i, r_i)$ and $\hat{\delta}_i = S_{\mathbf{w}}(\mathbf{p}_i, y_i) - S_{\mathbf{w}}(\mathbf{q}_i, y_i)$ for each $i \geq 1$. Then, for each $i \geq 1$,*

$$\mathbb{E} \left[\hat{\delta}_i \mid \mathcal{F}_{i-1} \right] = \delta_i. \quad (4.7)$$

The proof is provided in Appendix B.4. Lemma 4.1 shows that the condition for Theorems 3.1 and 3.2 also holds when comparing k -step-ahead forecasts according to the scoring rule (4.4), and thus we have a time-uniform CS for their average score differentials as well. We note that, at a stopping time τ , the resulting procedure will not take into account predictions of the future, say at time $\tau + k$ for some k , for which the actual outcome $y_{\tau+k}$ is not realized. This does not invalidate our procedure, as it would usually suffice to make comparisons based on realized outcomes only.

4.3 Mean Forecasts on Bounded Continuous Outcomes

Our derivation with binary outcomes and probability forecasts can also be extended to the case of forecasting the time-varying means of bounded continuous outcomes. In this case, reality is now assumed to choose an unknown distribution for the continuous outcome at each round t , such that the distribution has a time-varying mean parameter that the forecasters try to predict.¹¹ This generalizes the case of binary outcomes, in the sense that the unknown parameter r_t is in fact the mean of the outcome y_t given \mathcal{F}_{t-1} , as in (3.1). We now state the corresponding game to compare the case of bounded continuous outcomes with that of binary outcomes.

Game 4.3 (Sequentially Comparing Forecasts on Means of Bounded Continuous Outcomes). *Let $a, b \in \mathbb{R}$ such that $a < b$. For rounds $t = 1, 2, \dots$:*

1. *Forecaster 1 makes their mean forecast, $p_t \in [a, b]$.*
2. *Forecaster 2 makes their mean forecast, $q_t \in [a, b]$.*
3. *Reality chooses a distribution \mathcal{P}_t with mean $r_t \in [a, b]$. Note that \mathcal{P}_t (or r_t) is not revealed to the forecasters.*
4. *$y_t \sim \mathcal{P}_t$ is sampled and revealed to the forecasters.*

At each round t , forecasters can make their probability forecasts using any information available to them, including historical and previous outcomes $y_{-(H-1)}, \dots, y_0, y_1, \dots, y_{t-1}$, any of the previous forecasts made, p_1, \dots, p_{t-1} , q_1, \dots, q_{t-1} , as well as any other external information available to them. They cannot, however, make predictions based on any of the \mathcal{P}_t 's as well as information from the future.

¹¹Because the forecasters are assumed to predict the mean only, their forecasts are now viewed as deterministic, as opposed to probabilistic. In the case of binary outcomes, the two cases overlap, as the mean fully specifies the underlying distribution.

As with Game 3.1, Game 4.3 is inherently sequential, and there are no assumptions of parametric models or stationarity made on the underlying distribution for outcomes. The key difference between the two games, however, is that the forecasters in Game 4.3 are assumed to predict only the mean of the underlying distribution, \mathcal{P}_t , which may no longer be fully specified by its mean. This is to ensure that the martingale property of the sums of estimated and actual score differentials continues to hold; extending this to fully probabilistic forecasts for continuous outcomes remains future work. We are also implicitly adding the assumption that the underlying distribution of outcomes has a mean, an assumption that we did not need for the binary case.

Unlike in the binary or the categorical case, the boundedness assumption on forecasts and outcomes is required for the sub-exponential uniform boundaries we use in Theorem 3.2. An alternative is to only assume sub-Gaussianity of the score differentials $\hat{\delta}_i = S(p_i, y_i) - S(q_i, y_i)$ and use Theorem 3.1 instead.

Assuming boundedness or sub-Gaussianity, we can readily extend the definitions of score differentials (3.2) and (3.3) to the case of mean forecasts on continuous outcomes, and combine Lemma 3.1 with either Theorem 3.2 (boundedness) or 3.1 (sub-Gaussianity) to obtain a time-uniform CS for Δ_t .

4.4 Winkler’s Normalized Score Differentials

Focusing again on the case of binary outcomes, we now show that Theorems 3.1 and 3.2 can also be used to construct time-uniform CSs for a normalized version of average score differentials, also known as the Winkler score. Winkler (1994) provided a standardized scoring rule that measures the relative improvement of a given forecaster over an “unskilled” baseline forecaster, such as the historical average (referred to as *climatology* in weather forecasting) $c_t = c = \frac{1}{H} \sum_{h=-(H-1)}^0 y_h \forall t \geq 1$. This normalized version of the score can be viewed as a better reflection of the relative “skill” of a given forecaster (Winkler, 1994; Lai et al., 2011).

In our derivation, we slightly generalize the notion to allow any forecaster $(q_t)_{t=1}^\infty$ predictable w.r.t. $(\mathcal{F}_t)_{t=1}^\infty$ (and bounded away from 0 and 1) to be a baseline forecaster. For any $p, r \in [0, 1]$ and $q \in (0, 1)$, the *Winkler score* $w(p, q, r)$ can be defined as follows:

$$w(p, q, r) := \frac{S(p, r) - S(q, r)}{T(p, q)} \quad (4.8)$$

where $0/0 := 0$, and

$$\begin{aligned} T(p, q) &= S(p, \mathbf{1}(p \geq q)) - S(q, \mathbf{1}(p \geq q)) \\ &= [S(p, 1) - S(q, 1)] \mathbf{1}(p \geq q) + [S(p, 0) - S(q, 0)] \mathbf{1}(p < q) \end{aligned} \quad (4.9)$$

is a normalizer for the pointwise score differential.¹² Here, we fix S to be the Brier score. Note that $T(p, q) \geq 0$ and $T(p, q) = 0$ iff $p = q$ (in which case $w(p, q, r) = 0$), due to the propriety of S .

Winkler (1994) notes that, given a baseline forecaster $q = c$, w itself is a strictly proper scoring rule for p if S is strictly proper, which is the case when S is the Brier score. The score is standardized in the sense that, if the binary outcome is in fact generated according to

¹²We note that this normalizer also appears in its absolute value as the e-value increment in (Henzi and Ziegel, 2021), i.e., $E(\lambda) = 1 + \lambda \frac{S(p, r) - S(q, r)}{|T(p, q)|}$. This means that we can interpret the amount of wealth gained by betting against the null in (Henzi and Ziegel, 2021) reflects the relative skill score, as Winkler’s score does.

$y \sim \text{Ber}(p)$, then the expected score w.r.t. the outcome i.e., $\mathbb{E}_{y \sim \text{Ber}(p)}[w(p, q, y)]$, is minimized at zero for $p = q$ and maximized at 1 for $p = 0$ and $p = 1$.

We can now derive conditions for which we can also use Theorems 3.1 and 3.2 for the average of Winkler scores over time. For each time t , define $w_t = w(p_t, q_t, r_t)$ and $\hat{w}_t = w(p_t, q_t, y_t)$.

Lemma 4.2. *Suppose that, for each $t \geq 1$, $q_t \in (q_0, 1 - q_0)$ a.s. for some fixed $q_0 \in (0, 1)$. If S has a linear equivalent, then $\mathbb{E}[\hat{w}_t | \mathcal{F}_{t-1}] = w_t$ for each $i \geq 1$.*

The proof, provided in Appendix B.5, makes use of the fact that $(T(p_t, q_t))_{t=1}^\infty$ is predictable w.r.t. $(\mathcal{F}_t)_{t=1}^\infty$. The scalar q_0 determines the lower bound on the Winkler score. Given that S is the Brier score, the corresponding Winkler score has an upper bound of 1 and a lower bound of $1 - \frac{2}{q_0 \wedge (1 - q_0)}$ (happens when either $p = 0$ and $r = 1$ or $p = 1$ and $r = 0$).

We can now define the *average Winkler score* up to time t ,

$$W_t := \frac{1}{t} \sum_{i=1}^t w(p_i, q_i, r_i), \quad (4.10)$$

as well as its empirical estimate

$$\hat{W}_t := \frac{1}{t} \sum_{i=1}^t w(p_i, q_i, y_i), \quad (4.11)$$

for each $t \geq 1$. Then, by setting $\hat{\delta}_i \leftarrow \hat{w}_i$ and $\delta_i \leftarrow w_i$ in Theorem 3.1 or 3.2, we can also obtain a time-uniform CS for W_t . The average Winkler score W_t has an intuitive interpretation as a normalized version of the average score differential Δ_t in (3.2) or as the average “skill gap” between the two forecasters.

5 Experiments

In this section, we run both simulated and real-data experiments for sequential forecast comparison using our CSs as well as e-processes. All code and data sources for the experiments are made publicly available online at <https://github.com/yjchoe/ComparingForecasters>.

5.1 Simulated Experiments

As our first experiment, we empirically compare our CSs with the fixed-time CIs due to Lai et al. (2011) (Theorem 2). Importantly, the fixed-time CI is only valid at a time t fixed *a priori* and does not have a finite-sample coverage guarantee that the CS has. We also include an asymptotic CS, recently derived by Waudby-Smith et al. (2021) (Theorem 7), as another baseline. This CS can be viewed as the asymptotic analog of our non-asymptotic version in Theorem 3.2 and only has asymptotic guarantees. In practice, the asymptotic CS is expected to be the “limit” of the non-asymptotic CS, in the sense that the width of the non-asymptotic CS approaches the width of the asymptotic CS as t increases.

As for our simulated data, we generate a sequence of non-IID binary outcomes and compare different forecasters using our CS. It is natural to simulate the data following a similar protocol as Game 3.1, and we employ the following protocol throughout this experiment:

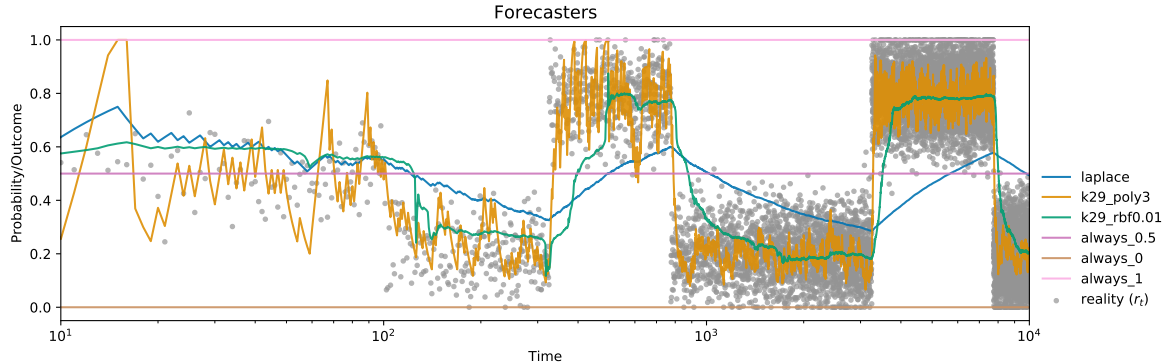


Figure 1: Various forecasters on a simulated non-IID data ($T = 10^4$) with sharp changepoints spaced out in log-scale. Note that, instead of plotting the binary outcomes $y_t \in \{0, 1\}$, we plot the reality sequence $(r_t)_{t=1}^T$ that generates the outcome sequence. See text for details about the forecasters.

Simulated Experiment Protocol. For each $t = 1, \dots, T$,

1. Forecaster 1 makes their forecast, $p_t \in [0, 1]$, using y_1, \dots, y_{t-1} .¹³
2. Forecaster 2 makes their forecast, $q_t \in [0, 1]$, using y_1, \dots, y_{t-1} .
3. Reality chooses a probability $r_t \in [0, 1]$. *This probability is not revealed to the forecasters.*
4. $y_t \sim \text{Ber}(r_t)$ is sampled and revealed to the forecasters.

At the end of each round t , we compute the $(1 - \alpha)$ -level Hoeffding and EB CS for Δ_t using Theorems 3.1 and 3.2 respectively. We use the Brier score $S(p, q) = -(p - q)^2$ as our default scoring rule, but we also explore other scoring rules later in the section.

To validate our approach, we compare several forecasters. These include constant baselines — $p_t = 0.5$ (`always_0.5`), $p_t = 0$ (`always_0`), and $p_t = 1$ (`always_1`) —, as well as the Laplace forecasting algorithm (`laplace`) $p_t = \frac{k+1}{t+1}$, where $k = \#\{i \in [t] : y_i = 1\}$. We also add predictions using the K29 defensive forecasting algorithm (Vovk et al., 2005), which is a game-theoretic forecasting method that leads to calibrated forecasts, using the polynomial kernel with degree $d = 3$ (`k29_poly3`), $K(p, q) = (1 + pq)^d$, and the Gaussian RBF kernel with noise $\sigma = 0.01$ (`k29_rbf0.01`), $K(p, q) = \exp\left(-\frac{(p-q)^2}{2\sigma^2}\right)$.

In Figure 1, we plot the reality sequence $(r_t)_{t=1}^T$ (gray dots), which is non-IID and contains sharp changepoints, as well as the probability forecasts made by various forecasters on the outcomes $(y_t)_{t=1}^T$ generated via $y_t \sim \text{Ber}(r_t)$ for each t . We set $T = 10^4$. The r_t 's are generated as follows:

$$r_t = [0.8 \cdot \theta_t + 0.2 \cdot (1 - \theta_t)] + \epsilon_t,$$

¹³The forecasters are allowed to also use any other information revealed up to time $t - 1$, such as forecasts made by other forecasters, but we do not include such a case in our simulated experiments. In reality, this is certainly a possible scenario.

where

$$\theta_t = \begin{cases} 0.5 & \text{for } t \in [1, 10^2] \\ 0 & \text{for } t \in (10^2, 0.5 \cdot 10^3] \\ 1 & \text{for } t \in (0.5 \cdot 10^3, 0.5 \cdot 10^4] \\ 0 & \text{for } t \in (0.5 \cdot 10^4, 10^4]. \end{cases}$$

and $\epsilon_t \sim \mathcal{N}(0, 0.1^2)$ is an independent Gaussian noise for each t .

Among the constant baselines, none of them are expected to dominate each other at the end, although the true Δ_t between them may change signs over time. For example, for $t \in (10^2, 0.5 \cdot 10^3)$, in which reality consistently favors the outcome 0, the `always_0` forecaster is expected to dominate over the `always_1` forecaster, although the sign will then reverse over the next span where reality consistently favors the outcome 1. Among the algorithmic forecasters, it is expected that the K29 variants will consistently perform better than the Laplace algorithm, especially when using ones with sharper kernels, because they should be better at modeling the sharp change points.

In Figure 2, we plot the 95% Hoeffding and EB CSs, fixed-time CI, and asymptotic CS for Δ_t (left), along with their widths (right). We draw these plots for three illustrative cases: when one forecaster is strictly better than the other always (top), when the two forecasters are alternately good but no better than the other overall (middle), and when one forecaster is typically but not always better than the other (bottom).

In all three cases, our CSs successfully cover Δ_t at any given time point, and their widths sharply decrease as more outcomes are observed. As expected, the width of the EB CS decays more quickly than the width of the Hoeffding CS. This trend, as well as the ratio between the width of the EB CS and its fixed-time counterpart, roughly matches the patterns observed in (Howard et al., 2021; Waudby-Smith et al., 2021). As noted before, the fixed-time CIs are only valid at a fixed time t and not uniformly over time, giving its tighter width. We also observe that the width of the EB CS approaches that of the asymptotic CS as time progresses ($t \geq 10^3$), matching our intuition that the asymptotic variant is a “limit” of our CS (which is also non-asymptotically valid). Finally, we see that the Hoeffding CS is much wider than the EB CS in the first and third cases, but not in the second case where Δ_t has sharp change points and the EB CS is wider. We suspect that this happens because the sharp change points contribute to having larger values of the intrinsic time \hat{V}_t for the EB CS, whereas the Hoeffding CS simply uses $\hat{V}_t = t$ irrespective of the variance process. Nevertheless, the widths of both CSs eventually reach the “limit” of the asymptotic CS, as t grows large.

In Figure 3, we now plot all pairwise comparisons between the constant baseline (`always_0.5`), the Laplace forecaster (`laplace`), and the K29 forecasters with the 3-degree polynomial kernel and the Gaussian RBF kernel with $\sigma = 0.01$ (`k29_poly3` and `k29_rbf0.01`, respectively). Overall, we find that the K29 forecasters all outperform the Laplace forecaster and the constant baseline, consistently across time. The Laplace forecaster and the constant baseline are also found to be no better than each other, as expected in this synthetic dataset. Between the two K29 forecasters, the ones using the 3-degree polynomial kernel eventually outperforms the one using the RBF kernel with $\sigma = 0.01$.

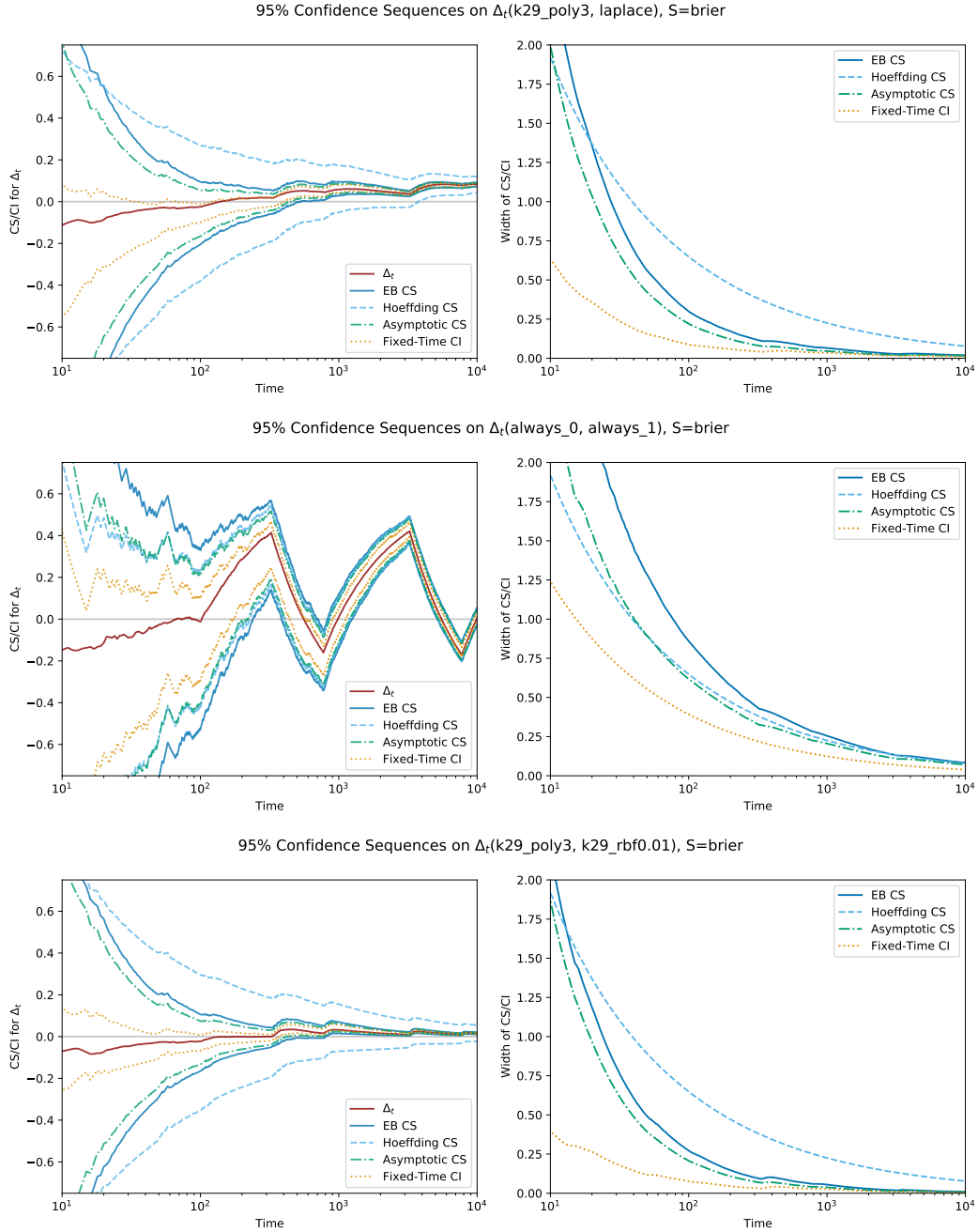


Figure 2: 95% EB CS (blue), Hoeffding-style CS (skyblue, dashed), asymptotic CS (green, dashdot), and fixed-time asymptotic CI (orange, dotted) for Δ_t (left), along with their widths (right), plotted for three different pairs of forecasts (top, middle, bottom). Scoring rule is the Brier score, and positive values of Δ_t indicate that the first forecaster is better than the second. Overall, the asymptotic CS is the tightest CS, followed by the EB CS and the Hoeffding CS. All three CSs cover Δ_t uniformly, and the width of the EB CS approaches that of the asymptotic CS as time grows large. The fixed-time CI is tighter than the CSs, but it does not have a stopping time guarantee. See text for further details.

95% Confidence Sequences on Δ_t , S=brier

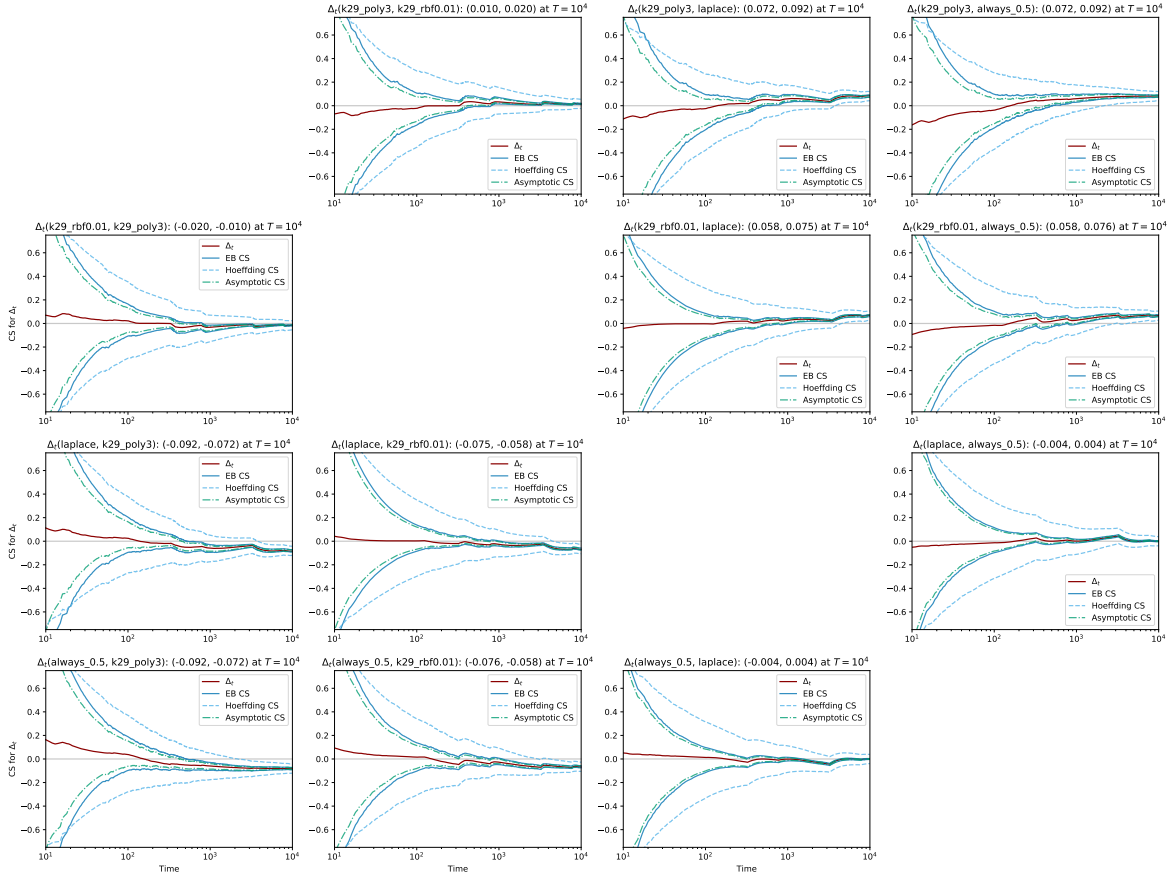


Figure 3: 95% confidence sequences on Δ_t between the constant baseline (always_0.5), the Laplace forecaster (laplace), and the K29 forecasters with different kernel functions (k29_poly3 and k29_rbf0.01). Scoring rule is the Brier score, and positive values of Δ_t indicate that the first forecaster is better than the second. As before, all three CSs cover Δ_t uniformly, and the width of the EB CS approaches that of the asymptotic CS as time grows large.

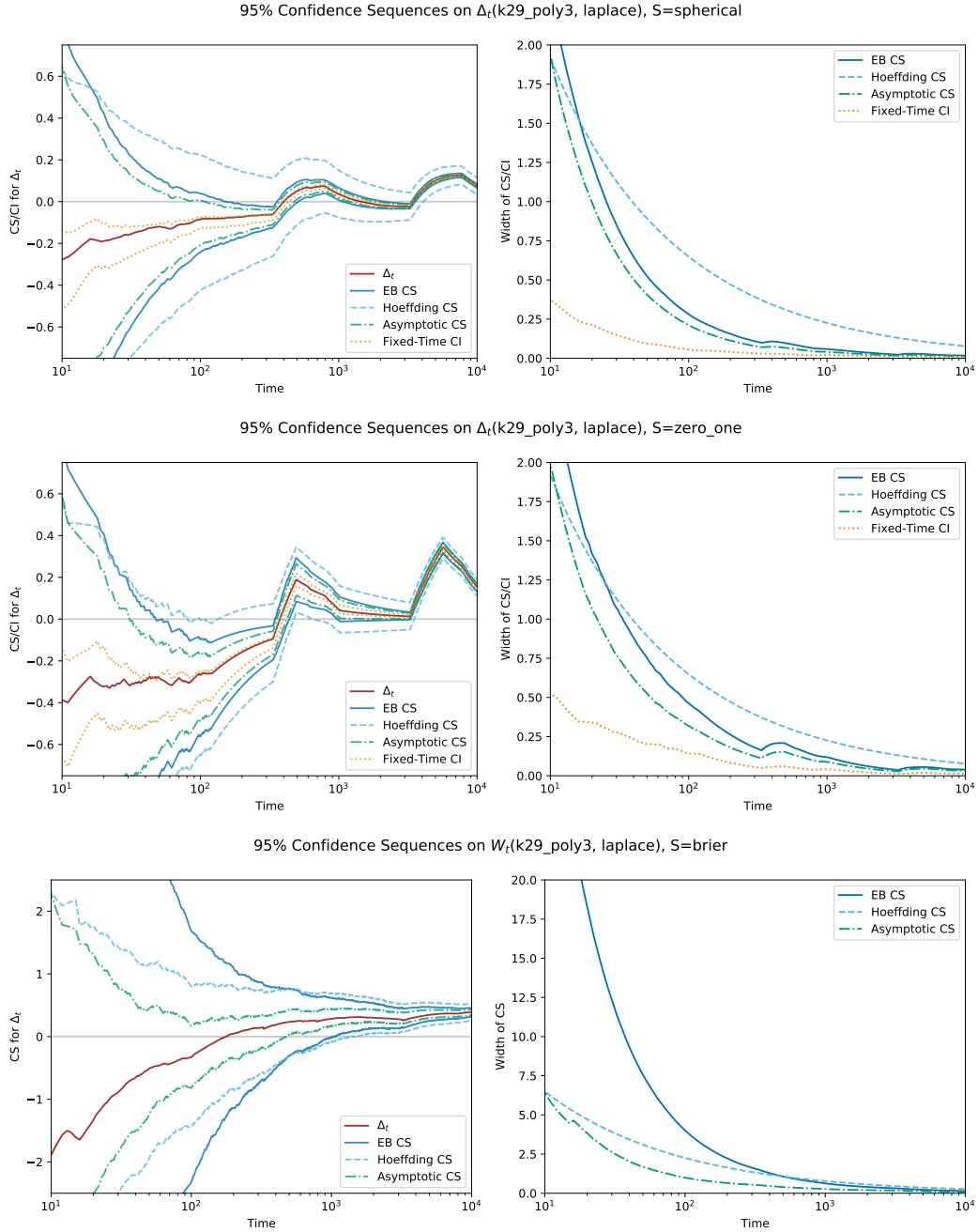


Figure 4: Comparing the use of different scoring rules on simulated data. Top and middle plots show the 95% CS on Δ_t between the K29 forecaster and the Laplace forecaster, using the spherical score and the zero-one score, respectively. Bottom plot shows the 95% CS on Winkler's score W_t of the K29 forecaster against the Laplace forecaster, truncated within values (0.1, 0.9). All scoring rules are defined to be positively oriented, such that positive values of Δ_t or W_t indicate that the first forecaster is better than the second. As in the case of the Brier score, all three CSs cover Δ_t uniformly, and the width of the EB CS approaches that of the asymptotic CS as time grows large.

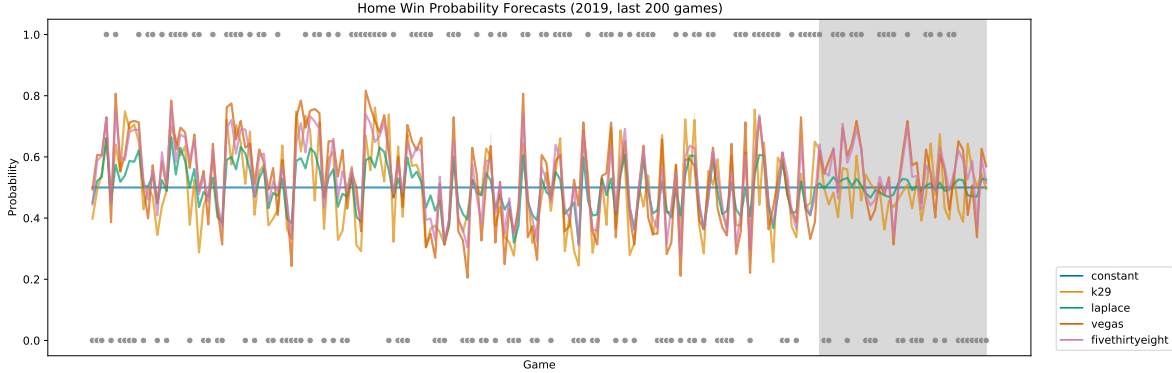


Figure 5: Various forecasters on the last 200 MLB games played in 2019 (including regular season and postseason). FiveThirtyEight and Vegas forecasts are publicly available forecasts online; Laplace and K29 forecasts are made using the historical outcomes as data without external information. *Note that the forecasts are computed using data from a 10-year window (2010 to 2019), but we only show the last year here for visualization purposes.* The shaded region highlights the playoffs (last seven being the World Series games).

Finally, in Figure 4, we plot the 95% CS for comparing the `k29_poly3` forecaster against the Laplace baseline, using the spherical score, the zero-one score, and the Winkler score (with the Brier score). Recall that the spherical score and the zero-one score are bounded and trivially have their linear equivalents, such that Lemma 3.1 holds, while the pointwise Winkler score satisfies the conditions of Lemma 4.2. For the average Winkler score, we additionally truncate the Laplace baseline into range $(0.1, 0.9)$ and use the bound $[1 - \frac{2}{0.1}, 1]$ on the pointwise Winkler scores. We observe that the 95% CS always covers the true Δ_t (or W_t) over time, and its width decreases similarly to the case of Brier scores and eventually approaches that of the asymptotic CS. These results illustrate that our CS can also be applied as long as one chooses a scoring rule that has a linear equivalent and has its score differentials bounded.

5.2 Comparing Forecasters on Major League Baseball Games

For a real-world application of our CSs, we consider the problem of predicting wins and losses for baseball games played in the Major League Baseball (MLB). Sports game prediction is particularly suitable for our setting, because there are several publicly available probability forecasts on the outcome of each game (e.g., FiveThirtyEight, betting odds, and pundits/experts), that are frequently updated across time. There is also no obvious assumption to be reasonably made about the outcome of the games, such as stationarity or assumptions of parametric models. Recall Table 1 for an illustration of forecasts made on MLB games.

We specifically focus on predicting the outcome of MLB games, recorded over ten years (2010-2019) culminating in the 2019 World Series between the Houston Astros and the Washington Nationals. We use every regular season and postseason MLB game from 2010 to 2019 as our dataset. We convert each game as a single time point in chronological order, leading to a total of $T = 25,165$ games. As for the forecasters, we consider the following:

- **fivethirtyeight**: Game-by-game probability forecasts on every MLB game since 1871, available on <https://data.fivethirtyeight.com/#mlb-elo>. According to the methodology report¹⁴, the probabilities are calculated using an ELO-based rating system for each team, and game-specific adjustments are made for the starting pitcher as well as other external factors (travel, rest, home field advantage, etc.). Before each new season, team ratings are reverted to the mean by one-third and combined with preseason projections from other outlets¹⁵.
- **vegas**: Pre-game closing odds made on each game by online sports bettors, as reported by <https://Vegas-Odds.com>.¹⁶ The betting odds are given in the American format, so each odds o is converted to its implied probability p via $p = \mathbf{1}(o \geq 0) \frac{100}{100+o} + \mathbf{1}(o < 0) \frac{-o}{100-o}$. Then, for each matchup¹⁷, the pair of implied probabilities for each team is rescaled to sum to 1. For example, given a matchup between team A and team B with betting odds $o_A = -140$ and $o_B = +120$, the implied probabilities are $\tilde{p}_A = 0.58$ and $\tilde{p}_B = 0.45$, and the rescaled probabilities are $p_A = 0.56$ and $p_B = 0.44$.
- **constant**: a constant baseline corresponding to $p_t = 0.5$ for each t .
- **laplace**: A seasonally adjusted Laplace algorithm, representing the season win percentage. Mathematically, it is given by $p_t = \frac{k_t + c_t}{n_t + 1}$, where k_t is the number of wins so far in the season, n_t is the number of games played in this season, and $c_t \in [0, 1]$ is a baseline that represents the final probability forecast from the previous season reverted to the mean by one-third. For example, if the previous season ended after round t_0 , then $k(t) = \sum_{i=t_0}^{t-1} \mathbf{1}(y_i = 1)$, $n(t) = t - t_0$, and $c_t = \frac{1}{3} \cdot p_{t_0} + \frac{2}{3} \cdot \frac{1}{2}$ (with $c_0 = \frac{1}{2}$).
- **k29**: The K29 algorithm using the 3-degree polynomial kernel, computed using data from the current season only.

In Figure 5, we plot the five probability forecasters on the last 200 games of 2019.

We perform all pairwise comparisons of the five aforementioned forecasters on the 10-year win/loss predictions. Note that we conduct this experiment as a *post-hoc* analysis, since all games have already been played — the only difference is that we can further optimize our uniform boundary to be the tightest at the final time step ($v_{\text{opt}} = \hat{V}_T$). Importantly, the procedure still takes into account that the games were forecast sequentially, and it still compares the forecasters in terms of their *predictive* performance by estimating $\Delta_t = (1/t) \sum_{i=1}^t \delta_i = (1/t) \sum_{i=1}^t \mathbb{E}[S(p_i, y_i) - S(q_i, y_i) \mid \mathcal{F}_{i-1}]$.

We plot the 95% Hoeffding, EB, and asymptotic CSs between all pairs of the five forecasters in Figure 6. We also list the 95% EB CS on the average score differential Δ_T as well as the average Winkler score W_T against the **laplace** baseline in Table 4. Our results suggest that the Laplace forecaster, representing a seasonally adjusted win percentage baseline, significantly outperforms all other forecasters we considered, in terms of the Brier score. This implies that neither of **fivethirtyeight** or **vegas** forecasts are better than the season-adjusted win percentage, which does not use any external information than the actual win/loss records. Even when we use the average Winkler score (Table 4(b)), we find that only the **vegas** forecasts are found to be not worse than the Laplace baseline. We also note from Figure 6 that the

¹⁴<https://fivethirtyeight.com/features/how-our-mlb-predictions-work/>

¹⁵Baseball Prospectus’s PECOTA, FanGraphs’ depth charts, and Clay Davenport’s predictions

¹⁶Download source: <https://sports-statistics.com/sports-data/mlb-historical-odds-scores-datasets/>

¹⁷In any given matchup, the sum of two implied probabilities is typically greater than 1, and the excess reflects the bettor’s profit margin (also known as overreach or vigorish).

Forecaster	95% EB CS	Forecaster	95% EB CS
<code>fivethirtyeight</code>	(-0.00982, -0.00664)	<code>fivethirtyeight</code>	(-0.07002, -0.01255)
<code>vegas</code>	(-0.00840, -0.00478)	<code>vegas</code>	(-0.04684, 0.01086)
<code>k29</code>	(-0.03550, -0.02939)	<code>k29</code>	(-0.21450, -0.15076)
<code>constant</code>	(-0.01727, -0.01419)	<code>constant</code>	(-0.18004, -0.12685)

(a) Δ_T (using Brier) against `laplace`(b) W_T against `laplace`

Table 4: 95% EB CS on the average score differential Δ_T (using Brier) and the average Winkler score W_T , against the `laplace` forecaster as a baseline ($T = 25, 165$). Positive (negative) values of Δ_T or W_T indicate that the forecaster is better (worse) than the baseline. All forecasters are found to perform worse than the `laplace` forecaster using both the Brier score and the Winkler score at time T , except for the `vegas` forecaster using the Winkler score.

`vegas` forecaster is found to outperform the `fivethirtyeight` forecaster at $T = 25, 165$, while both forecasters at $T = 25, 165$ are found to outperform the `constant` baseline that always predicts $p_t = 0.5$.

To further interpret our results, recall that the Brier score is a strictly proper scoring rule, which encodes both calibration and sharpness of the forecasts (Winkler et al., 1996; Gneiting and Raftery, 2007). Because both the `fivethirtyeight` and `vegas` forecasts are sharper than the `laplace` forecaster, as shown in Figure 5, we can infer that the `fivethirtyeight` and `vegas` suffer more in terms of calibration, which the Laplace forecaster achieves (it is the “least skillful” calibrated forecaster, borrowing the phrase from Winkler et al. (1996)). These results highlight the difficulty of making forecasts on the outcome of sports games that are both calibrated and sharp.

Finally, note that we can re-compute the CSs with a pre-specified value of v_{opt} , such that they remain valid in the scenario where one starts from $t = 1$ and continuously collect data compare forecasts as time progresses. For example, a skeptic who compares `fivethirtyeight` and `laplace` forecasters after each game can decide, after some time τ at which the entire CS falls below zero, that the latter outperforms the former, without having to worry about “sampling to a foregone conclusion” (Anscombe, 1954). The skeptic can also use the CSs to find, for instance, that the `vegas` forecaster is better than the `fivethirtyeight` going into Game 7 of the 2019 World Series, by observing that the 95% EB CS for $\Delta_t(\text{vegas}, \text{fivethirtyeight})$ at time $T - 1$ is entirely less than zero.

95% Confidence Sequences on Δ_r , $S=brier$

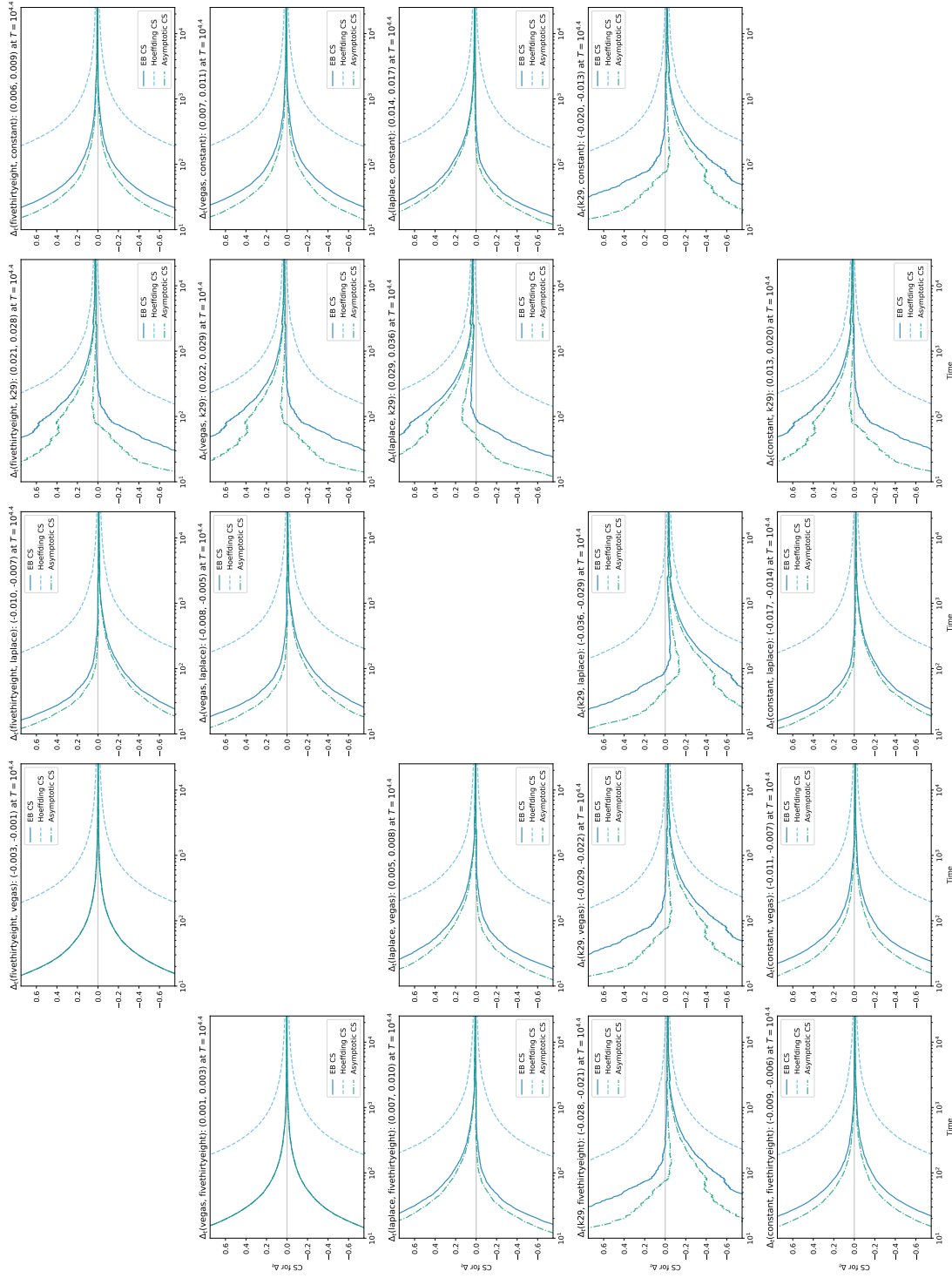


Figure 6: Comparing MLB win probability forecasts from 2010 to 2019, using our CSs as well as the asymptotic CS at significance level $\alpha = 0.05$. $T = 25, 165 \approx 10^{4.4}$ corresponds to the final game of the 2019 World Series. Note that the horizontal axis is drawn in log-scale. The Brier score is used. We find that, over time, none of the other forecasters outperform the Laplace forecaster (third row/column), which corresponds to the season-adjusted win percentage.

5.3 Comparing Statistical Postprocessing Methods for Weather Forecasts

As our second real-data experiment and an illustration of our e-processes derived in Section 3.5, we compare a set of statistical postprocessing methods for weather forecasts (Vannitsem et al., 2021), following recent work by Henzi and Ziegel (2021). Statistical postprocessing here refers to the process of correcting for biases and dispersion errors in ensemble weather forecasts, which are produced by perturbing the initial conditions of numerical weather prediction (NWP) methods. As ensemble forecasts are commonly used in state-of-the-art weather forecasting systems as a means of producing probabilistic forecasts, statistical postprocessing is considered a key component of modern weather forecasting.

In their work, Henzi and Ziegel (2021) compare statistical postprocessing methods for predicting the Probability of Precipitation (PoP) using the ensemble forecast data from the European Centre for Medium-Range Weather Forecasts (ECMWF; Molteni et al. (1996)). The dataset includes the observed 24-hour precipitation from January 06, 2007 to January 01, 2017 at four airport locations (Brussels, Frankfurt, London Heathrow, and Zurich), and for each location and date it also includes 1- to 5-day ensemble forecasts, consisting of a high resolution forecast, 50 perturbed ensemble forecasts at a lower resolution, and a control run for the perturbed forecasts. They consider three statistical postprocessing methods in their experiments: isotonic distributional regression (IDR; Henzi et al. (2021)) and heteroscedastic censored logistic regression (HCLR; Messner et al. (2014)), as well as a variant of HCLR without its scale parameter (HCLR_). Each method is applied to the first-half of the data, separately for each airport location and lag $h = 1, \dots, 5$, and the second-half data is used to make sequential comparisons of the postprocessing methods. Note that each location has a different number of observations: 3,406 for Brussels, 3,617 for Frankfurt, 2,256 for London, and 3,241 for Frankfurt. See Section 5 in Henzi et al. (2021) and Section 5.1 in Henzi and Ziegel (2021) for further details about the dataset and the postprocessing methods. In Figure 7, we plot the three postprocessing methods for 1-day PoP forecasts for one of the airport locations (Brussels) in the final year (January 01, 2016 to January 01, 2017).

Our main goal here is to sequentially compare the three statistical postprocessing methods using our EB CS from Theorem 3.2. As noted in Sections 1.1 and 3.5, the inferential conclusions drawn from our CS are different than those from Henzi and Ziegel (2021), who provide a test of *step-by-step* conditional forecast dominance instead of *average*. While rejecting the null in the e-value-based sequential test only tells us that there exists some time point where one forecaster outperforms another, finding that our CS for the average score differentials is away from zero tells us that one forecaster tends to outperform another in predicting the next outcome. As such, if we were to convert our CS into its corresponding sequential test, we would expect our version to have a larger null set and thus reject less the null often. On the other hand, the two methods are similar in that they both come with anytime-valid guarantees, in particular at arbitrary stopping times, such that one can “safely” (Johari et al., 2015; Grünwald et al., 2019) update their conclusions as more data is collected.

In Figure 8, we plot both the 90% EB CS on Δ_t (top) as well as the corresponding sub-exponential e-values for the weak one-sided null H_0^w (bottom), between HCLR and IDR, IDR and HCLR_, and HCLR and HCLR_ on 1-day PoP forecasts, using the Brier score. Note that these are the same three pairs compared in Figure 3 of Henzi and Ziegel (2021), which would correspond to e-values for the strong one-sided null H_0^s . The EB CS is computed using Theorem 3.2 and the gamma-exponential CM boundary from Lemma 3.2; the e-values are then computed using Theorem 3.3 and the exponential supermartingale that constructs the gamma-exponential CM boundary for the CS, as described in Section 3.5. We use the same

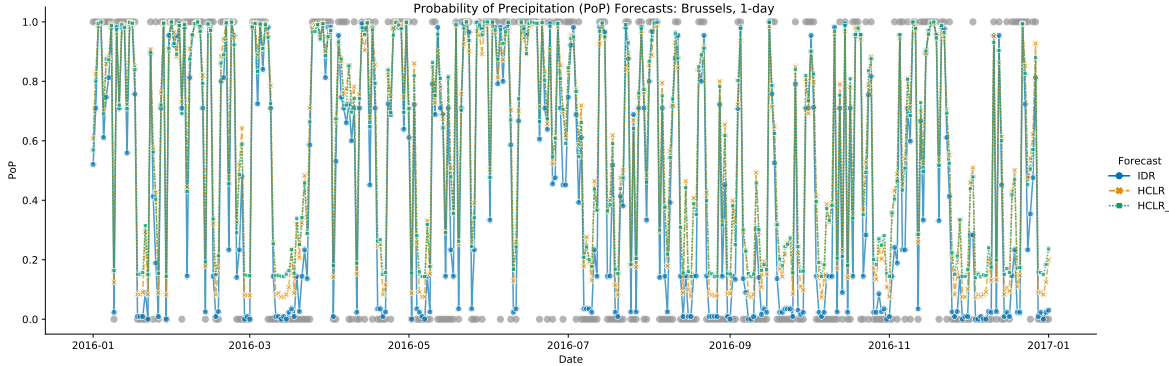


Figure 7: Comparing three statistical postprocessing methods (IDR, HCLR, HCLR_) for ensemble weather forecasts on the Probability of Precipitation (PoP). The binary outcome is drawn as gray dots. For visualization purposes, we plot the data and the forecasts only for the final year (January 01, 2016 to January 01, 2017) and at one airport location (Brussels) with lag 1.

set of hyperparameters ($c = 0.1$, $v_{\text{opt}} = 0.5$, and $\rho = \frac{v_{\text{opt}}}{W_{-1}(\alpha^2/e)+1}$ with $\alpha = 0.1$, following Proposition 3(a) in Howard et al. (2021)) for both the CS and the e-values, as they rely on the same underlying supermartingale. Here we choose the significance level of $\alpha = 0.1$, because it roughly corresponds to the threshold of 10 for e-values to be considered a “strong” evidence against the null (Vovk and Wang, 2021).

We first note from Figure 8 that the lower bound of our 90% EB CSs on $\Delta_t(p, q)$ and the e-values for $H_0^w : \Delta_t(p, q) \leq 0$ share a similar trend over time, where e-values grow large when the lower bound grows significantly larger than zero, implying that the forecaster p is better than the forecaster q . Whereas the CSs provide a (two-sided) estimate of $\Delta_t(p, q)$ with uncertainty, the e-values explicitly give the amount of evidence for whether one is better than the other. In this way, the two procedures complement each other for the purpose of sequentially valid inference on Δ_t . We finally note that, while the e-values are defined for one-sided nulls on $\Delta_t(p, q)$, we can also compute the e-values for $H_0^w : \Delta_t(q, p) \leq 0$, and they would correspond to the upper bound of the EB CSs.

In terms of the inferential conclusions based on 1-day forecasts, we find from the 90% CSs that IDR forecasts are found to outperform both HCLR and HCLR_ 1-day forecasts for Brussels, and that HCLR forecasts outperform HCLR_ forecasts for Frankfurt and Zurich, but we do not find significant differences at other locations between other pairs. Our e-values (with a threshold at 10) also lead to the same conclusions, and they also more clearly visualize at which point in time is one forecaster first found to outperform the other and how that pattern changes (e.g., when comparing IDR to HCLR_ for Brussels, IDR is found to be better as early as 2012, and it also shows the period between late 2012 and late 2015 where it is no longer found to be better, before eventually regaining evidence favoring IDR starting 2016).

When we compare our e-values for the weak null H_0^w with the e-values for the strong null H_0^s provided by Henzi and Ziegel (2021) (Figure 3), we find that e-values for the strong null are large whenever e-values for the weak null are also large, but not vice versa. Specifically, the comparisons of IDR against HCLR_ and HCLR against HCLR_ in Frankfurt are only found to have strong evidence against the strong null, but not the weak null. This is consistent with our previous discussion in Section 3.5 that the strong null implies the weak null and thus is easier to “reject” (or gather more evidence against), although rejecting the weak null is more

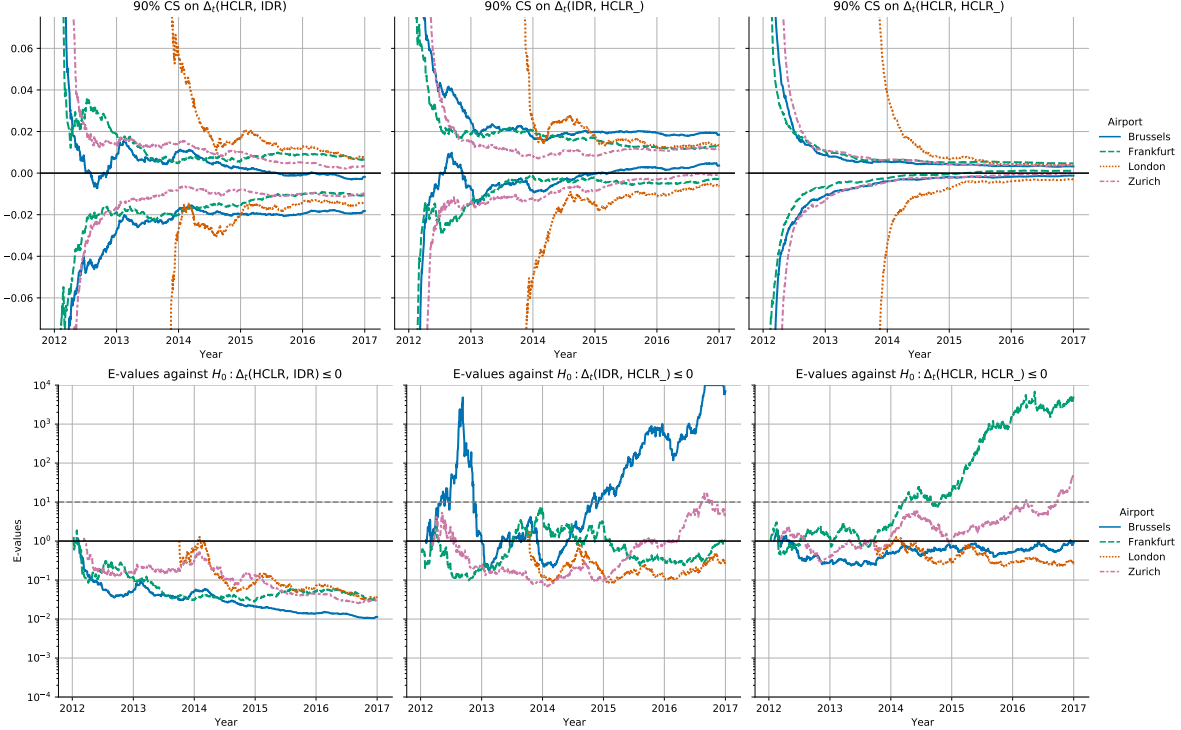


Figure 8: (Top) 90% EB CSs for Δ_t between pairs of statistical postprocessing methods (HCLR and IDR; IDR and HCLR_; HCLR and HCLR_) for 1-day ensemble forecasts using Theorem 3.2, computed and plotted separately for each airport: Brussels ($T = 1,703$), Frankfurt ($T = 1,809$), London ($T = 1,128$), and Zurich ($T = 1,621$). Note that positive/negative scores of $\Delta_t(\mathbf{p}, \mathbf{q})$ indicates that forecaster \mathbf{p} is better/worse than forecaster \mathbf{q} . Overall, the CSs capture the time-varying score gap on average between the two forecasters across the years. (Bottom) E-values for the null that $H_0^w: \Delta_t \leq 0$, corresponding to (the lower bound of) the 90% CSs above. These e-values are the *weak* or *average* counterpart to Henzi and Ziegel (2021)’s e-values for the *strong* or *step-by-step* null that $H_0^s: \delta_i \leq 0 \forall i = 1, \dots, t$. Note that the e-values exceed 10 approximately when the lower bound of the 90% CS exceeds 0. Both procedures use the Brier score as the scoring rule. See text for further details.

informative as it provides a cumulative comparison over time. For example, in Frankfurt, we can infer we only have strong evidence that IDR has outperformed HCLR_ *at some point in time* between 2012 and 2017, but we do not have sufficient evidence that IDR has outperformed HCLR_ *on a typical day* in the same time period.

In Table 5, we further compare the e-values for the weak null (E^w) and the strong null (E^s), evaluated at the last time step T (January 01, 2017) for each location and lag $(1, \dots, 5)$, where T corresponds to January 01, 2017. Here, we also find that e-values for the weak null are large mostly when e-values for the strong null are large. Using an e-value threshold of 10, there are a total of 22 out of 60 comparisons where E^s is large, compared to only 16 for E^w . The conclusions overlap for 11 comparisons, and all 5 comparisons for which only E^w exceeds 10 are those between HCLR and HCLR_, suggesting that HCLR forecasts seem to perform better than HCLR_ when compared using the average score differentials. Conversely, 9 out of 11 comparisons for which only E^s exceeds 10 are those between IDR and HCLR_, suggesting that there is less evidence that HCLR_ outperforms IDR when compared using the average

Location	Lag	HCLR/IDR		IDR/HCLR		HCLR/HCLR	
		E^w	E^s	E^w	E^s	E^w	E^s
Brussels	1	0.011	0	> 100	> 100	0.915	> 100
	2	0.021	0.01	2.426	> 100	1.871	13.602
	3	0.056	0.425	0.142	> 100	15.606	15.185
	4	1.307	4.804	0.021	1.943	4.078	5.165
	5	58.929	16.969	0.015	0.415	54.825	3.436
Frankfurt	1	0.031	0	1.079	> 100	> 100	> 100
	2	0.020	0.054	71.817	> 100	> 100	> 100
	3	0.021	0.078	> 100	> 100	> 100	26.569
	4	0.297	2.291	0.065	9.618	> 100	5.54
	5	0.829	1.526	0.029	2.362	8.285	3.227
London	1	0.037	0.029	0.247	14.979	0.262	2.845
	2	0.028	0.188	0.625	> 100	0.184	2.868
	3	0.043	0.734	0.262	40.905	0.228	2.488
	4	0.141	1.429	0.076	1.7	0.753	1.744
	5	0.375	1.577	0.034	0.379	0.249	1.118
Zurich	1	0.031	0.003	4.973	> 100	56.612	61.747
	2	0.049	0.116	0.903	36.891	> 100	10.276
	3	0.301	1.516	0.091	31.924	> 100	5.098
	4	3.788	4.069	0.031	1.276	18.219	2.771
	5	> 100	15.151	0.021	0.842	> 100	2.383

Table 5: E-values between pairs of statistical postprocessing methods for ensemble weather forecasts across different locations and lags, where T is the last time step (January 01, 2017). E^w indicates e-values for the weak null $H_0^w(p, q) : \Delta_t(p, q) \leq 0$, computed using Theorem 3.3; E^s indicates e-values for the strong null $H_0^s(p, q) : \delta_i(p, q) \leq 0 \forall i = 1, \dots, t$, computed by Henzi and Ziegel (2021). Both procedures use the Brier score as the scoring rule. “q/p” indicates CS on $\Delta_T(p, q)$. Across different locations and lags, E^s is large (greater than 10) at 22 location-lag pairs, compared to 16 for E^w (11 of which overlap). See text for further details.

score differentials (for E^w). Together, we see that E^w gives less evidence than E^s that HCLR can perform as well as or better than IDR or HCLR. Finally, we also include the 90% EB CSs on Δ_T in Table 6, which is consistent with the e-values for the weak null in Table 5 but further provides a symmetric comparison between pairs of forecasters.

6 Conclusions

In this work, we derived time-uniform CSs that allow us to sequentially compare the quality of probability forecasts at arbitrary stopping times. These CSs require no distributional assumptions on the sequence of outcomes, such as stationarity, or on how the forecasts are generated. We also derived e-processes and anytime-valid p-processes that correspond to our CSs, and also discussed several extensions of our CSs, including forecasts on categorical outcomes, k -step-ahead forecasts, mean forecasts on sub-Gaussian continuous outcomes, and Winkler’s normalized score. We’ve empirically illustrated the validity of the CSs on synthetic data and showed their applications to real-world baseball forecasts and weather forecasts. In doing so, we also provided comparisons with fixed-time CIs (Lai et al., 2011) that are invalid at stopping

Location	Lag	HCLR/IDR	IDR/HCLR	HCLR/HCLR
Brussels	1	(-0.018, -0.002)	(0.004, 0.018)	(-0.001, 0.003)
	2	(-0.013, 0.004)	(-0.002, 0.014)	(-0.001, 0.004)
	3	(-0.010, 0.011)	(-0.006, 0.012)	(-0.000, 0.006)
	4	(-0.003, 0.017)	(-0.014, 0.005)	(-0.001, 0.006)
	5	(0.001, 0.019)	(-0.016, 0.001)	(0.000, 0.006)
Frankfurt	1	(-0.011, 0.006)	(-0.003, 0.013)	(0.001, 0.005)
	2	(-0.013, 0.003)	(0.001, 0.015)	(0.001, 0.006)
	3	(-0.013, 0.004)	(0.001, 0.016)	(0.002, 0.007)
	4	(-0.004, 0.011)	(-0.007, 0.007)	(0.001, 0.006)
	5	(-0.003, 0.013)	(-0.010, 0.004)	(-0.000, 0.005)
London	1	(-0.014, 0.008)	(-0.006, 0.013)	(-0.003, 0.004)
	2	(-0.016, 0.006)	(-0.004, 0.015)	(-0.004, 0.005)
	3	(-0.013, 0.008)	(-0.006, 0.012)	(-0.004, 0.005)
	4	(-0.008, 0.013)	(-0.009, 0.008)	(-0.002, 0.007)
	5	(-0.006, 0.016)	(-0.013, 0.005)	(-0.004, 0.005)
Zurich	1	(-0.010, 0.003)	(-0.001, 0.011)	(0.000, 0.004)
	2	(-0.008, 0.006)	(-0.003, 0.010)	(0.001, 0.004)
	3	(-0.004, 0.010)	(-0.006, 0.007)	(0.001, 0.005)
	4	(-0.001, 0.012)	(-0.010, 0.003)	(-0.000, 0.005)
	5	(0.002, 0.015)	(-0.011, 0.000)	(0.001, 0.006)

Table 6: 90% EB CS on Δ_T between pairs of statistical postprocessing methods for ensemble weather forecasts across different locations and lags, where T is the last time step (January 01, 2017). “q/p” indicates CS on $\Delta_T(p, q)$. We use the Brier score as the scoring rule. Note that positive values of $\Delta_T(p, q)$ indicates that p outperforms q . The CSs give estimates of $\Delta_T(p, q)$ with uncertainty, and they provide a symmetric comparison of the forecasters unlike the e-values.

times and cannot be sequentially tracked, as well as more recent e-values that were developed for a strong null (Henzi and Ziegel, 2021), rather than our more preferable weak null.

Acknowledgements

AR acknowledges funding from NSF DMS 1916320. Research reported in this paper was sponsored in part by the DEVCOM Army Research Laboratory under Cooperative Agreement W911NF-17-2-0196 (ARL IoBT CRA). The views and conclusions contained in this document are those of the authors and should not be interpreted as representing the official policies, either expressed or implied, of the Army Research Laboratory or the U.S. Government. The U.S. Government is authorized to reproduce and distribute reprints for Government purposes notwithstanding any copyright notation herein. YJC and AR thank Ruodu Wang and Glenn Shafer, who were coinstructors with AR on a tri-university game-theoretic statistical inference course, for which this paper started off as a course project.

References

- Anscombe, F. J. (1954). Fixed-sample-size analysis of sequential observations. *Biometrics*, 10(1):89–100.
- Brier, G. W. (1950). Verification of forecasts expressed in terms of probability. *Monthly weather review*, 78(1):1–3.
- Darling, D. A. and Robbins, H. (1967). Confidence sequences for mean, variance, and median. *Proceedings of the National Academy of Sciences of the United States of America*, 58(1):66.
- Dawid, A. P. (1984). Statistical theory: the prequential approach. *Journal of the Royal Statistical Society: Series A (General)*, 147(2):278–290.
- DeGroot, M. H. and Fienberg, S. E. (1983). The comparison and evaluation of forecasters. *Journal of the Royal Statistical Society: Series D (The Statistician)*, 32(1-2):12–22.
- Diebold, F. X. and Mariano, R. S. (1995). Comparing predictive accuracy. *Journal of Business & Economic Statistics*, 13(3).
- Doob, J. L. (1940). Regularity properties of certain families of chance variables. *Transactions of the American Mathematical Society*, 47(3):455–486.
- Ehm, W. and Krüger, F. (2018). Forecast dominance testing via sign randomization. *Electronic Journal of Statistics*, 12(2):3758–3793.
- Fan, X., Grama, I., and Liu, Q. (2015). Exponential inequalities for martingales with applications. *Electronic Journal of Probability*, 20.
- Garthwaite, P. H., Kadane, J. B., and O’Hagan, A. (2005). Statistical methods for eliciting probability distributions. *Journal of the American Statistical Association*, 100(470):680–701.
- Giacomini, R. and White, H. (2006). Tests of conditional predictive ability. *Econometrica*, 74(6):1545–1578.
- Gneiting, T., Balabdaoui, F., and Raftery, A. E. (2007). Probabilistic forecasts, calibration and sharpness. *Journal of the Royal Statistical Society: Series B (Statistical Methodology)*, 69(2):243–268.
- Gneiting, T. and Raftery, A. E. (2007). Strictly proper scoring rules, prediction, and estimation. *Journal of the American statistical Association*, 102(477):359–378.
- Good, I. (1971). Comment on “Measuring information and uncertainty” by Robert J. Buehler. *Foundations of Statistical Inference*, pages 337–339.
- Good, I. J. (1952). Rational decisions. *Journal of the Royal Statistical Society: Series B (Methodological)*, 14(1):107–114.
- Grünwald, P., de Heide, R., and Koolen, W. (2019). Safe testing. *arXiv preprint arXiv:1906.07801*.
- Henzi, A. and Ziegel, J. F. (2021). Valid sequential inference on probability forecast performance. *arXiv preprint arXiv:2103.08402*.

- Henzi, A., Ziegel, J. F., and Gneiting, T. (2021). Isotonic distributional regression. *Journal of the Royal Statistical Society: Series B (Statistical Methodology)*.
- Hoeffding, W. (1963). Probability inequalities for sums of bounded random variables. *Journal of the American Statistical Association*, 58(301):13–30.
- Howard, S. R., Ramdas, A., McAuliffe, J., and Sekhon, J. (2020). Time-uniform chernoff bounds via nonnegative supermartingales. *Probability Surveys*, 17:257–317.
- Howard, S. R., Ramdas, A., McAuliffe, J., and Sekhon, J. (2021). Time-uniform, nonparametric, nonasymptotic confidence sequences. *The Annals of Statistics*, 49(2):1055 – 1080.
- Jamieson, K. and Jain, L. (2018). A bandit approach to multiple testing with false discovery control. In *Proceedings of the 32nd International Conference on Neural Information Processing Systems*, pages 3664–3674.
- Jamieson, K., Malloy, M., Nowak, R., and Bubeck, S. (2014). lil’UCB: An optimal exploration algorithm for multi-armed bandits. In *Conference on Learning Theory*, pages 423–439. PMLR.
- Jennison, C. and Turnbull, B. W. (1989). Interim analyses: the repeated confidence interval approach. *Journal of the Royal Statistical Society: Series B (Methodological)*, 51(3):305–334.
- Johari, R., Pekelis, L., and Walsh, D. J. (2015). Always valid inference: Bringing sequential analysis to A/B testing. *arXiv preprint arXiv:1512.04922*.
- Karampatziakis, N., Mineiro, P., and Ramdas, A. (2021). Off-policy confidence sequences. In Meila, M. and Zhang, T., editors, *Proceedings of the 38th International Conference on Machine Learning*, volume 139 of *Proceedings of Machine Learning Research*, pages 5301–5310. PMLR.
- Lai, T. L. (1976a). Boundary crossing probabilities for sample sums and confidence sequences. *The Annals of Probability*, pages 299–312.
- Lai, T. L. (1976b). On confidence sequences. *The Annals of Statistics*, 4(2):265–280.
- Lai, T. L., Gross, S. T., and Shen, D. B. (2011). Evaluating probability forecasts. *The Annals of Statistics*, 39(5):2356–2382.
- Lehmann, E. L. (1975). *Nonparametrics: statistical methods based on ranks*. Holden-day.
- Messner, J. W., Mayr, G. J., Wilks, D. S., and Zeileis, A. (2014). Extending extended logistic regression: Extended versus separate versus ordered versus censored. *Monthly Weather Review*, 142(8):3003–3014.
- Molteni, F., Buizza, R., Palmer, T. N., and Petroliagis, T. (1996). The ECMWF ensemble prediction system: Methodology and validation. *Quarterly journal of the royal meteorological society*, 122(529):73–119.
- Ramdas, A., Ruf, J., Larsson, M., and Koolen, W. (2020). Admissible anytime-valid sequential inference must rely on nonnegative martingales. *arXiv preprint arXiv:2009.03167*.

- Ramdas, A., Ruf, J., Larsson, M., and Koolen, W. M. (2021). Testing exchangeability: Fork-convexity, supermartingales and e-processes. *International Journal of Approximate Reasoning*.
- Robbins, H. (1970). Statistical methods related to the law of the iterated logarithm. *The Annals of Mathematical Statistics*, 41(5):1397–1409.
- Robbins, H. and Siegmund, D. (1970). Boundary crossing probabilities for the wiener process and sample sums. *The Annals of Mathematical Statistics*, pages 1410–1429.
- Rosenbaum, P. R. (1995). *Observational studies*. Springer.
- Schervish, M. J. (1989). A general method for comparing probability assessors. *The Annals of Statistics*, 17(4):1856 – 1879.
- Shafer, G. (2021). Testing by betting: A strategy for statistical and scientific communication. *Journal of the Royal Statistical Society: Series A (Statistics in Society)*, 184(2):407–431.
- Shafer, G. and Vovk, V. (2019). *Game-Theoretic Foundations for Probability and Finance*, volume 455. John Wiley & Sons.
- Vannitsem, S., Bremnes, J. B., Demaeyer, J., Evans, G. R., Flowerdew, J., Hemri, S., Lerch, S., Roberts, N., Theis, S., and Atencia, A. (2021). Statistical postprocessing for weather forecasts: Review, challenges, and avenues in a big data world. *Bulletin of the American Meteorological Society*, 102(3):E681–E699.
- Ville, J. (1939). Etude critique de la notion de collectif. *Bull. Amer. Math. Soc*, 45(11):824.
- Vovk, V., Takemura, A., and Shafer, G. (2005). Defensive forecasting. In *International Workshop on Artificial Intelligence and Statistics*, pages 365–372. PMLR.
- Vovk, V. and Wang, R. (2021). E-values: Calibration, combination and applications. *The Annals of Statistics*, 49(3):1736 – 1754.
- Wainwright, M. J. (2019). *High-dimensional statistics: A non-asymptotic viewpoint*, volume 48. Cambridge University Press.
- Waudby-Smith, I., Arbour, D., Sinha, R., Kennedy, E. H., and Ramdas, A. (2021). Doubly robust confidence sequences for sequential causal inference. *arXiv preprint arXiv:2103.06476*.
- Waudby-Smith, I. and Ramdas, A. (2020). Estimating means of bounded random variables by betting. *arXiv preprint arXiv:2010.09686*.
- Winkler, R. L. (1994). Evaluating probabilities: Asymmetric scoring rules. *Management Science*, 40(11):1395–1405.
- Winkler, R. L., Munoz, J., Cervera, J. L., Bernardo, J. M., Blattenberger, G., Kadane, J. B., Lindley, D. V., Murphy, A. H., Oliver, R. M., and Ríos-Insua, D. (1996). Scoring rules and the evaluation of probabilities. *Test*, 5(1):1–60.
- Wu, J. and Ding, P. (2020). Randomization tests for weak null hypotheses in randomized experiments. *Journal of the American Statistical Association*, pages 1–16.
- Zhao, S., Zhou, E., Sabharwal, A., and Ermon, S. (2016). Adaptive concentration inequalities for sequential decision problems. *Advances in Neural Information Processing Systems*, 29:1343–1351.

A Tight Confidence Sequences via Uniform Boundaries

The confidence sequences we derive in this work rely on the tight CSs derived in Howard et al. (2021) using the technique of time-uniform Chernoff bounds via uniform boundaries (Howard et al., 2020). Here, we briefly summarize the key definitions required for deriving our CSs.

Let $(S_t)_{t=0}^\infty$, $(V_t)_{t=0}^\infty$ be real-valued processes adapted to $(\mathcal{F}_t)_{t=0}^\infty$ with $S_0 = V_0 = 0$ and $V_t \geq 0$ for all t . S_t can be thought of as a summary statistic accumulated up to time t , such as $\bar{X}_t = \sum_{i=1}^t X_i$, and $(V_t)_{t=0}^\infty$ as an intrinsic time measured by the variance accumulated up to time t . Further, let $\psi : [0, \lambda_{\max}) \rightarrow \mathbb{R}$ be a cumulant generative function (CGF) of a random variable, such as a standard Gaussian, an exponential, or a gamma. A working example throughout the paper is the exponential CGF: $\psi_{E,c}(\lambda) = c^{-2}(-\log(1 - c\lambda) - c\lambda)$ for $c > 0$. We denote $\psi_E = \psi_{E,1}$.

We say that $(S_t)_{t=0}^\infty$ is *sub- ψ with variance process* $(V_t)_{t=0}^\infty$ if, for each $\lambda \in [0, \lambda_{\max})$, there exists a supermartingale $(L_t(\lambda))_{t=0}^\infty$ with respect to $(\mathcal{F}_t)_{t=0}^\infty$ such that $\mathbb{E}[L_0(\lambda)] \leq 1$ and

$$\exp\{\lambda S_t - \psi(\lambda)V_t\} \leq L_t(\lambda) \text{ a.s. for all } t. \quad (\text{A.1})$$

Let $\mathbb{S}_\psi = \{((S_t, V_t))_{t=0}^\infty : (S_t)_{t=0}^\infty \text{ is sub-}\psi \text{ with variance process } (V_t)_{t=0}^\infty\}$. Then, a function $u : \mathbb{R} \rightarrow \mathbb{R}$ is a *sub- ψ uniform boundary with crossing probability* $\alpha \in (0, 1)$ for scale $c \in \mathbb{R}$ if

$$\sup_{(S_t, V_t) \in \mathbb{S}_\psi} \mathbb{P}(\exists t \geq 1 : S_t \geq u(V_t)) \leq \alpha. \quad (\text{A.2})$$

These uniform boundaries based on exponential supermartingales provide time-uniform and non-asymptotic bounds for summary statistics regardless of the underlying distributional assumptions. In this work, we will utilize sub-exponential uniform boundaries, i.e., sub- ψ uniform boundaries with $\psi_{E,c}(\lambda) = c^{-2}(-\log(1 - c\lambda) - \lambda)$ for some $c \in \mathbb{R}$, that are used to derive tight confidence sequences in Howard et al. (2021).

B Proofs

B.1 Proof of Lemma 3.1

The definition of linear equivalents and this (simple) lemma are due to Lai et al. (2011). Let \tilde{S} be a linear equivalent of S . By its linearity on its second argument and by (3.1), we have that, for each i ,

$$\mathbb{E}[\tilde{S}(p_i, y_i) \mid \mathcal{F}_{i-1}] = \tilde{S}(p_i, r_i). \quad (\text{B.1})$$

Also, let $d(r) := S(p, r) - \tilde{S}(p, r)$ be the function that does not depend on p . Then, for each i ,

$$S(p_i, r_i) - S(q_i, r_i) = [\tilde{S}(p_i, r_i) + d(r_i)] - [\tilde{S}(q_i, r_i) - d(r_i)] = \tilde{S}(p_i, r_i) - \tilde{S}(q_i, r_i). \quad (\text{B.2})$$

Combining (B.1) and (B.2) gives us the result.

B.2 Proof of Theorem 3.2

The proof closely resembles the proof of Theorem 4 in Howard et al. (2021). Fix $c = 1$ without loss of generality, so that $\hat{\delta}_i$, δ_i , and γ_i are each bounded by $[-\frac{1}{2}, \frac{1}{2}]$ and consequently the differences $\hat{\delta}_i - \delta_i$ and $\hat{\delta}_i - \gamma_i$ are bounded by $[-1, 1]$.

Our goal is to show that

$$L_t(\lambda) = \exp \left\{ \lambda S_t - \psi_E(\lambda) \sum_{i=1}^t (\hat{\delta}_i - \gamma_i)^2 \right\} \quad (\text{B.3})$$

is a supermartingale for each $\lambda \in [0, 1)$, where $\psi_E(\lambda) = \psi_{E,1}(\lambda) = -\log(1 - \lambda) - \lambda$.

Let $Y_i = \hat{\delta}_i - \delta_i$ and $Z_i = \gamma_i - \delta_i$, such that $Y_i - Z_i = \hat{\delta}_i - \gamma_i \in [-1, 1]$. Using the fact that $\exp \{ \lambda \xi - \psi_E(\lambda) \xi^2 \} \leq 1 + \lambda \xi$ for all $\lambda \in [0, 1)$ and $\xi \geq -1$ (Fan et al., 2015), we have

$$\exp \left\{ \lambda (Y_i - Z_i) - \psi_E(\lambda) (Y_i - Z_i)^2 \right\} \leq 1 + \lambda (Y_i - Z_i).$$

Multiplying each side by $e^{\lambda Z_i}$, we get

$$\exp \left\{ \lambda Y_i - \psi_E(\lambda) (Y_i - Z_i)^2 \right\} \leq e^{\lambda Z_i} (1 - \lambda Z_i) + \lambda e^{\lambda Z_i} Y_i.$$

Now, conditional on \mathcal{F}_{i-1} , we know that $\mathbb{E}[Y_i | \mathcal{F}_{i-1}] = \mathbb{E}[\hat{\delta}_i - \delta_i | \mathcal{F}_{i-1}] = 0$ by the first condition. We also know that $(Z_i)_{i=1}^\infty$ is predictable w.r.t. $(\mathcal{F}_i)_{i=1}^\infty$, as $(\gamma_i)_{i=1}^\infty$, $(p_i)_{i=1}^\infty$, $(q_i)_{i=1}^\infty$, $(r_i)_{i=1}^\infty$ are all predictable w.r.t. $(\mathcal{F}_i)_{i=1}^\infty$. Thus, by taking conditional expectations on both sides, and substituting back $Y_i = \hat{\delta}_i - \delta_i$ and $Z_i = \gamma_i - \delta_i$ on the left-hand side, we get

$$\begin{aligned} \mathbb{E} \left[\exp \left\{ \lambda (\hat{\delta}_i - \delta_i) - \psi_E(\lambda) (\hat{\delta}_i - \gamma_i)^2 \right\} \middle| \mathcal{F}_{i-1} \right] &\leq e^{\lambda Z_i} (1 - \lambda Z_i) + \lambda e^{\lambda Z_i} \mathbb{E}[Y_i | \mathcal{F}_{i-1}] \\ &= e^{\lambda Z_i} (1 - \lambda Z_i) \leq 1, \end{aligned}$$

using $1 - x \leq e^{-x}$ for the final inequality.

Finally, observe that the left-hand side is precisely the expected increment of $(L_t(\lambda))_{t=1}^\infty$ at time t . It follows that $\mathbb{E}[L_t(\lambda) | \mathcal{F}_{t-1}] \leq L_{t-1}(\lambda)$, i.e., $(L_t(\lambda))_{t=1}^\infty$ is a supermartingale. Thus, by (A.1) and (A.2), we have

$$\mathbb{P} \left(\exists t \geq 1 : S_t \geq u(\hat{V}_t) \right) \leq \alpha \quad (\text{B.4})$$

for a sub- ψ_E (i.e., sub-exponential) uniform boundary u with crossing probability $\alpha/2$ and scale $c = 1$. Using the fact that $\frac{1}{t} S_t = \frac{1}{t} \sum_{i=1}^t \hat{\delta}_i - \frac{1}{t} \sum_{i=1}^t \delta_i = \hat{\Delta}_t - \Delta_t$, we can divide each side of the inequality by t to obtain the upper confidence bound. Finally, by applying the same argument to $(-S_t, \hat{V}_t)$ and combining the upper and lower bounds with a union bound, we obtain the CS:

$$\mathbb{P} \left(\forall t \geq 1 : \left| \hat{\Delta}_t - \Delta_t \right| < \frac{u(\hat{V}_t)}{t} \right) \geq 1 - \alpha. \quad (\text{B.5})$$

B.3 Proof of Theorem 3.3

Let $S_t = \sum_{i=1}^t (\hat{\delta}_i - \delta_i) = t(\hat{\Delta}_t - \Delta_t)$ and $\hat{V}_t = \sum_{i=1}^t (\hat{\delta}_i - \gamma_i)^2$ where $(\gamma_i)_{i=1}^\infty$ is predictable w.r.t. $(\mathcal{F}_i)_{i=1}^\infty$. As shown in the proof of Theorem 3.2 (Appendix B.2), we have that, for any $\lambda \in [0, \lambda_{\max})$,

$$L_t(\lambda) := \exp \left\{ \lambda S_t - \psi_E(\lambda) \hat{V}_t \right\} \quad (\text{B.6})$$

is a supermartingale w.r.t. $(\mathcal{F}_t)_{t=1}^\infty$, that is, $\mathbb{E}[L_t(\lambda) | \mathcal{F}_{t-1}] \leq L_{t-1}(\lambda)$ for each t .

Now, under $H_0^w(p, q)$, we have that $\exp\{-\lambda \sum_{i=1}^t \delta_i\} \geq 1$, so

$$\begin{aligned} L_t(\lambda) &= \exp\left\{\lambda \sum_{i=1}^t \hat{\delta}_i - \psi_E(\lambda) \hat{V}_t\right\} \exp\left\{-\lambda \sum_{i=1}^t \delta_i\right\} \\ &\geq \exp\left\{\lambda \sum_{i=1}^t \hat{\delta}_i - \psi_E(\lambda) \hat{V}_t\right\} = E_t(\lambda). \end{aligned} \quad (\text{B.7})$$

Note that $(E_t(\lambda))_{t=1}^\infty$ is adapted to $(\mathcal{F}_t)_{t=1}^\infty$. Because $L_t(\lambda)$ is a supermartingale w.r.t. $(\mathcal{F}_t)_{t=1}^\infty$, it then follows that, under H_0^w , at any stopping time τ ,

$$\mathbb{E}[E_\tau(\lambda)] \leq \mathbb{E}[L_\tau(\lambda)] \leq 1 \quad (\text{B.8})$$

where the last inequality follows from Doob's optional stopping theorem (Doob, 1940) and that $L_0(\lambda) = 1$ vacuously.

B.4 Proof of Lemma 4.1

Let \tilde{S} be a linear equivalent of S . Define \tilde{S}_w as follows:

$$\tilde{S}_w(\mathbf{p}_t, r_t) := \sum_{k=1}^K w_k \tilde{S}(p_t^{(k)}, r_t). \quad (\text{B.9})$$

Then, \tilde{S}_w is a linear equivalent of S_w , as for any \mathbf{p} and r , $\tilde{S}(\mathbf{p}, r)$ is a linear function of r and $S(\mathbf{p}, r) - \tilde{S}(\mathbf{p}, r) = \sum_{k=1}^K w_k [S(p^{(k)}, r) - \tilde{S}(q^{(k)}, r)]$ does not depend on \mathbf{p} .

We now show the analogs of (B.1) and (B.2) using the linearity of sums in S_w and \tilde{S}_w . First note that, because $p_t^{(k)}$ is a forecast made at the beginning of round $t - k + 1$, it only uses information available to forecasters up to time $t - k$, i.e., $p_t^{(k)} \in \mathcal{G}_{t-k}$. (For example, $p_t^{(1)} \in \mathcal{G}_{t-1}$, i.e., 1-step ahead forecasts are predictable w.r.t. $(\mathcal{G}_t)_{t=1}^\infty$, consistent with our previous formulation in Section 3.2.) It then follows that $(p_t^{(k)})_{t=1}^\infty$ is predictable w.r.t. $(\mathcal{G}_t)_{t=1}^\infty$ and $(\mathcal{F}_t)_{t=1}^\infty$ for each k , as $p_t^{(k)} \in \mathcal{G}_{t-k} \subseteq \mathcal{G}_{t-1} \subsetneq \mathcal{F}_{t-1}$. This gives us the analog of (B.1):

$$\mathbb{E}\left[\tilde{S}_w(\mathbf{p}_t, y_t) \mid \mathcal{F}_{t-1}\right] = \sum_{k=1}^K w_k \mathbb{E}\left[\tilde{S}(p_t^{(k)}, y_t) \mid \mathcal{F}_{t-1}\right] = \sum_{k=1}^K w_k \tilde{S}(p_t^{(k)}, r_t) = \tilde{S}_w(\mathbf{p}_t, r_t). \quad (\text{B.10})$$

Also, analogous to (B.2), we have that

$$\begin{aligned} S_w(\mathbf{p}_t, r_t) - S_w(\mathbf{q}_t, r_t) &= \sum_{k=1}^K w_k [S(p_t^{(k)}, r_t) - \tilde{S}(q_t^{(k)}, r_t)] \\ &= \sum_{k=1}^K w_k \left[\left(\tilde{S}(p_t^{(k)}, r_t) + d(r_t) \right) - \left(\tilde{S}(q_t^{(k)}, r_t) - d(r_t) \right) \right] \\ &= \sum_{k=1}^K w_k [\tilde{S}(p_t^{(k)}, r_t) - \tilde{S}(q_t^{(k)}, r_t)] \\ &= \tilde{S}_w(\mathbf{p}_t, r_t) - \tilde{S}_w(\mathbf{q}_t, r_t) \end{aligned} \quad (\text{B.11})$$

where $d(r) := S(p, r) - \tilde{S}(p, r)$ is the function that does not depend on p .

Given (B.10) and (B.11), the proof of Theorem 3.2 can readily be extended to derive the analogous confidence sequences for average forecast score differentials under S_w . We state this extension as a corollary.

B.5 Proof of Lemma 4.2

First, observe that $(T(p_t, q_t))_{t=1}^\infty$ is predictable w.r.t. $(\mathcal{F}_t)_{t=1}^\infty$, since $T(p_t, q_t) \in \mathcal{G}_{t-1} \subsetneq \mathcal{F}_{t-1}$. This means that the equivalent of (B.1) holds for (4.8):

$$\begin{aligned} \mathbb{E}[w(p_t, q_t, y_t) \mid \mathcal{F}_{t-1}] &= \frac{\mathbb{E}[S(p_t, y_t) - S(q_t, y_t) \mid \mathcal{F}_{t-1}]}{T(p_t, q_t)} \\ &= \frac{\mathbb{E}[\tilde{S}(p_t, y_t) - \tilde{S}(q_t, y_t) \mid \mathcal{F}_{t-1}]}{T(p_t, q_t)} \\ &= \frac{\tilde{S}(p_t, r_t) - \tilde{S}(q_t, r_t)}{T(p_t, q_t)} \\ &= \frac{S(p_t, r_t) - S(q_t, r_t)}{T(p_t, q_t)} = w(p_t, q_t, r_t), \end{aligned}$$

where we use (B.2) in the second and fourth equalities and (B.1) in the third equality. Note that the score differences are bounded by a value that depends on both q_0 and S . For the Brier score, this bound is given by $\left[-\frac{2}{q_0}, \frac{2}{q_0}\right]$.

C Computing the Gamma-Exponential Mixture

Here, we derive the gamma-exponential mixture corresponding to the e-process for the weak null, as discussed in Section 3.5. By Proposition 9 in Howard et al. (2021), the expression for the gamma-exponential mixture is given by

$$m(s, v) := \frac{\left(\frac{\rho}{c^2}\right)^{\frac{\rho}{c^2}}}{\Gamma\left(\frac{\rho}{c^2}\right) P\left(\frac{\rho}{c^2}, \frac{\rho}{c^2}\right)} \frac{\Gamma\left(\frac{v+\rho}{c^2}\right) P\left(\frac{v+\rho}{c^2}, \frac{cs+v+\rho}{c^2}\right)}{\left(\frac{cs+v+\rho}{c^2}\right)^{\frac{v+\rho}{c^2}}} \exp\left\{\frac{cs+v}{c^2}\right\}, \quad (\text{C.1})$$

where $\Gamma(a, z) := \int_z^\infty u^{a-1} e^{-u} du$ is the upper incomplete gamma function, $\Gamma(a) := \Gamma(a, 0)$ is the gamma function, and P is the regularized lower incomplete gamma function defined as

$$P(a, z) := \frac{1}{\Gamma(a)} \int_0^z u^{a-1} e^{-u} du \quad (\text{C.2})$$

for $a, z > 0$. Note that both Γ and P can be computed efficiently in standard scientific computing software.¹⁸

In the following, we derive the expression (C.1) and show its upper bound in the case where $s + v + \rho < 0$. For notational simplicity, we assume $c = 1$, but an analogous proof can be made for any $c > 0$.

Recall that $\psi_E(\lambda) = -\log(1 - \lambda) - \lambda$ for $\lambda \in [0, 1)$. Using the gamma density $f_\rho(\lambda) =$

¹⁸E.g., P can be computed using `boost::math::gamma_p` in C++ and `scipy.special.gammainc` in Python.

$C(\rho)(1 - \lambda)^{\rho-1}e^{-\rho(1-\lambda)}$, where $C(\rho) = \frac{\rho^\rho}{P(\rho,\rho)\Gamma(\rho)}$, we have that, for $\rho > 0$,

$$\begin{aligned}
m(s, v) &= C(\rho) \int_0^1 \exp \{ \lambda s - \psi_E(\lambda) v \} \cdot (1 - \lambda)^{\rho-1} e^{-\rho(1-\lambda)} d\lambda \\
&= C(\rho) \int_0^1 e^{\lambda(s+v)} (1 - \lambda)^v \cdot (1 - \lambda)^{\rho-1} e^{-\rho(1-\lambda)} d\lambda \\
&= C(\rho) \int_0^1 (1 - \lambda)^{v+\rho-1} e^{\lambda(s+v)-\rho(1-\lambda)} d\lambda \\
&= C(\rho) \left(\int_0^1 (1 - \lambda)^{v+\rho-1} e^{-(s+v+\rho)(1-\lambda)} d\lambda \right) e^{s+v}, \tag{C.3}
\end{aligned}$$

where in the last equality we used

$$\lambda(s + v) - \rho(1 - \lambda) = (s + v) - (1 - \lambda)(s + v) - (1 - \lambda)\rho = -(s + v + \rho)(1 - \lambda) + (s + v).$$

Now, let $a = v + \rho$ and $z = s + v + \rho$, and note that $a > 0$.

If $z > 0$, then using the change-of-variable formula $u = (s + v + \rho)(1 - \lambda) = z(1 - \lambda)$, we have that

$$\begin{aligned}
m(s, v) &= C(\rho) \left(\int_z^0 \left(\frac{u}{z} \right)^{a-1} e^{-u} \frac{du}{-z} \right) e^{s+v} \\
&= C(\rho) \cdot \frac{1}{z^a} \left(\int_0^z u^{a-1} e^{-u} du \right) e^{s+v} \tag{C.4}
\end{aligned}$$

$$= C(\rho) \frac{\Gamma(a)P(a, z)}{z^a} e^{s+v}, \tag{C.5}$$

where we use the fact that the integral in (C.4) corresponds to the numerator of the lower incomplete gamma function $P(a, z)$ in (C.2). The expression (C.5) can be computed in closed-form.

On the other hand, if $z < 0$, then using the change-of-variable formula $u = -(s + v + \rho)(1 - \lambda) = -z(1 - \lambda)$, we obtain

$$\begin{aligned}
m(s, v) &= C(\rho) \left(\int_{-z}^0 \left(\frac{u}{-z} \right)^{a-1} e^u \frac{du}{z} \right) e^{s+v} \\
&= C(\rho) \cdot \frac{1}{(-z)^a} \left(\int_0^{-z} u^{a-1} e^u du \right) e^{s+v} \\
&= C(\rho) \cdot \frac{1}{|z|^a} \left(\int_0^{|z|} u^{a-1} e^u du \right) e^{s+v}. \tag{C.6}
\end{aligned}$$

Although the integral in (C.6) is no longer a regularized lower gamma function, we can still

show that $m(s, v)$ as a whole is bounded by e . Since $e^u \leq e^{|z|} = e^{-z}$ for $u \leq |z|$, we have that

$$\begin{aligned} m(s, v) &\leq C(\rho) \cdot \frac{1}{|z|^a} \left(\int_0^{|z|} u^{a-1} du \right) e^{-z} \cdot e^{s+v} \\ &= C(\rho) \cdot \frac{1}{|z|^a} \left(\int_0^{|z|} u^{a-1} du \right) e^{-\rho} \end{aligned} \tag{C.7}$$

$$\begin{aligned} &= C(\rho) \cdot \frac{1}{|z|^a} \left(\frac{u^a}{a} \right) \Big|_0^{|z|} e^{-\rho} \\ &= \frac{C(\rho)e^{-\rho}}{v + \rho}, \end{aligned} \tag{C.8}$$

where in (C.7) we used $-z + (s + v) = -(s + v + \rho) + (s + v) = -\rho$, and in (C.8) we substituted in $a = v + \rho$. We can further bound this value, using the fact that $v > 0$ and substituting back in $C(\rho)$:

$$\begin{aligned} m(s, v) &\leq \frac{C(\rho)e^{-\rho}}{v + \rho} \leq \frac{C(\rho)e^{-\rho}}{\rho} \\ &= \rho^{\rho-1} e^{-\rho} \cdot \left(\int_0^\rho u^{\rho-1} e^{-u} du \right)^{-1} \\ &\leq \rho^{\rho-1} e^{-\rho} \cdot \left(e^{-\rho} \int_0^\rho u^{\rho-1} du \right)^{-1} \end{aligned} \tag{C.9}$$

$$\begin{aligned} &= \rho^{\rho-1} \cdot \left[\left(\frac{u^\rho}{\rho} \right) \Big|_0^\rho \right]^{-1} \\ &= 1, \end{aligned} \tag{C.10}$$

where in (C.9) we used the fact that $e^{-\rho} \leq e^{-u}$ for $u \in [0, \rho]$. It makes sense that $m(s, v)$ is upper-bounded by 1 when $z = s + v + \rho < 0$, because $s < -(v + \rho) < 0$ would imply that the sum of score differentials is negative, which is an evidence that supports the weak null. In our implementation, we use the upper bound (C.8), which can be computed easily and gets substantially smaller than 1 when $v + \rho \gg 0$.

D Comparing CS Widths on IID Means

To validate and finetune our CSs, we compare the widths of various time-uniform CS applicable to the mean of independent and identically distributed (IID) random variables. We compare both the Hoeffding-style (H) CS (Theorem 3.1 and the empirical-Bernstein (EB) CS (Theorem 3.2) using both the conjugate-mixture (CM) and the polynomial stitching uniform boundaries, as described in Section 3.4. We also include predictable-mixed confidence sequences, namely the predictably-mixed Hoeffding (PM-H) CS and empirical Bernstein (PM-EB) CS from [Waudby-Smith and Ramdas \(2020\)](#), which are time-uniform CS that are also applicable for means of IID random variables. We also include the asymptotic CS described in [Waudby-Smith et al. \(2021\)](#). As for the data, we use the difference between two i.i.d. Beta random variables, as a proxy for score differentials between two sets of forecasts: for $i = 1, \dots, 10,000$,

$$\delta_i \stackrel{\text{IID}}{\sim} \text{Beta}(30, 10) - \text{Beta}(10, 30). \tag{D.1}$$

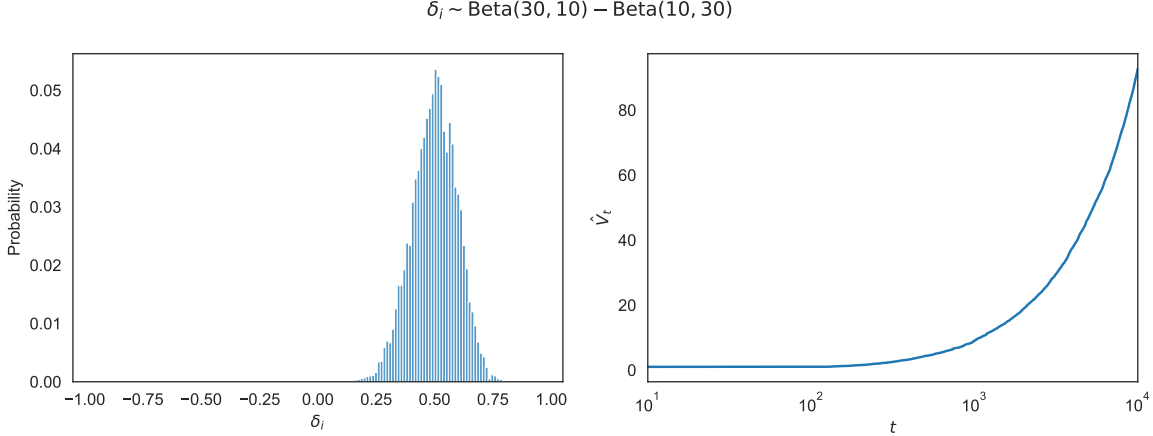


Figure 9: (Left) Histogram of $\delta_i \stackrel{\text{IID}}{\sim} \text{Beta}(30, 10) - \text{Beta}(10, 30)$ for $i = 1, \dots, 10,000$. (Right) Plot of the intrinsic time $\hat{V}_t = \sum_{i=1}^t (\delta_i - \hat{\Delta}_{i-1})^2$, where $\hat{\Delta}_{i-1} = \sum_{j=1}^{i-1} \hat{\delta}_j$. Note that the horizontal axis t is drawn in log-scale. Also note that the hyperparameter v_{opt} determines the intrinsic time \hat{V}_t at which the uniform boundary is the tightest.

Note that $-1 \leq \delta_i \leq 1$ a.s. and that $\mathbb{E}[\delta_i] = \frac{30}{30+10} - \frac{10}{10+30} = \frac{1}{2}$. Figure 9 illustrates the data sampled according to (D.1) (left) as well as the intrinsic time $\hat{V}_t = \sum_{i=1}^t (\hat{\delta}_i - \hat{\Delta}_{i-1})^2$, where $\hat{\Delta}_{i-1} = \sum_{j=1}^{i-1} \hat{\delta}_j$, over time (right). Note that, when choosing the uniform boundary for the CSs, the hyperparameter v_{opt} determines the intrinsic time \hat{V}_t at which the width of the uniform boundary is the tightest (Proposition 3, Howard et al. (2021)).

In Figure 10 (left), we present the hyperparameter tuning results of the CM-EB CS with respect to its optimal intrinsic time parameter v_{opt} , which corresponds to the point in the variance process where the boundary is the tightest. As a point of comparison, we also plot the polynomial stitching EB CS with hyperparameters $v_{\text{opt}} = 10$, $s = 1.4$, and $\eta = 2$. Comparing the values of $v_{\text{opt}} \in \{0.1, 1, 10, 100, 1000\}$, we find that the CM-EB CS is the tightest across time (up to $T = 10^4$) with $v_{\text{opt}} = 10$. Based on these results, we use the CM-EB CS with $v_{\text{opt}} = 10$ for our other experiments throughout the paper (except for the baseball experiments, which we conduct as a post-hoc analysis using the sample variance from the data).

In Figure 10 (right), we plot the widths of the different kinds of time-uniform CS, optimized for the intrinsic time $v_{\text{opt}} = 10$ when applicable. Generally speaking, we observe that the CSs are the tightest for the asymptotic CS, followed by the EB CS variants and the Hoeffding CS variants. This is consistent with our intuition, as the EB CS additionally makes use of the estimated variance to achieve smaller widths than the Hoeffding CS, and the asymptotic CS is the “limit” of EB CS in terms of the width while sacrificing the non-asymptotic guarantee (Waudby-Smith et al., 2021). For the EB CS variants, the CM-EB CS is tighter towards the beginning ($t < 10^3$) while the PM-EB CS becomes slightly tighter afterwards, and the stitching CS is not as tight as the other two. This is also as expected, as the CM-EB and PM-EB CS have similar widths (up to differences determined by the choice of hyperparameters) (Waudby-Smith and Ramdas, 2020) and the stitching CS tends to be looser in practice (Howard et al., 2021). This trend is also analogous for the Hoeffding CS variants, although the stitching variant does become tighter for larger t in this case.

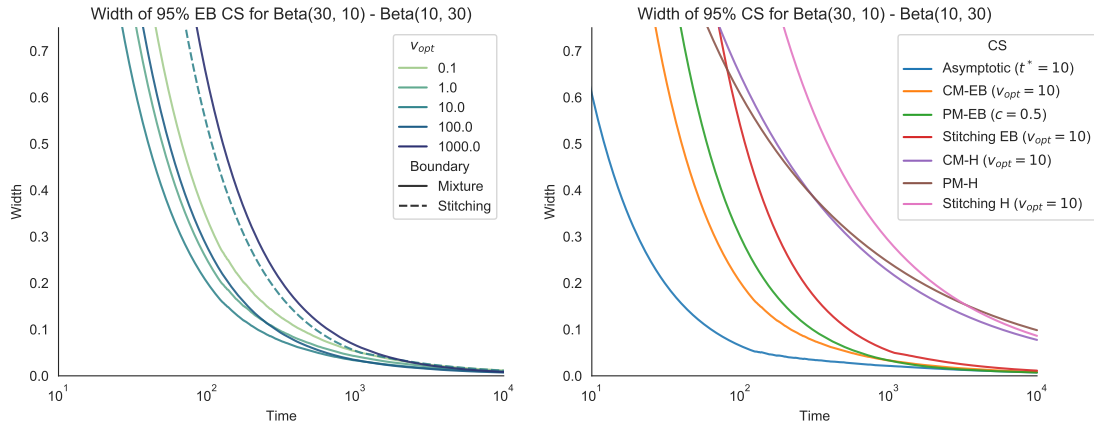


Figure 10: (Left) Hyperparameter tuning for the width of CM-EB CS by adjusting the optimal intrinsic time parameter v_{opt} . The choice $v_{opt} = 10$ gives the smallest width overall, although $v_{opt} = 100$ is comparable for $t > 10^3$. The width of stitching EB CS (with $v_{opt} = 1$) is also drawn as a point of comparison. (Right) Comparing the widths of different types of time-uniform CS. Overall, the asymptotic CS is the tightest, followed by the EB variants and then by the Hoeffding variants.